Sulfate Land Application Enhances Biodegradation in a Petroleum Hydrocarbon Smear Zone

by Kanwartej S. Sra, Violaine Ponsin, Ravi Kolhatkar, Daniel Hunkeler, Neil R. Thomson, Eugene L. Madsen, and Timothy Buscheck

Kanwartej S Sra - Chevron Technical Center,Houston,Texas,United States

Violaine Ponsin - Université du Québec à Montréal,Montreal,Quebec,Canada

Ravi V. Kolhatkar - Chevron Technical Center,Houston,Texas,United States

Daniel Hunkeler - University of Neuchatel,Centre for Hydrogeology and Geothermics,Neuchatel,Switzerland

Neil R. Thomson - University of Waterloo,Department of Civil and Environmental Engineering,Waterloo,Ontario,Canada

Eugene Madsen - Cornell Unversity,Ithaca,New York,United States

Timothy Buscheck - San Ramon,United States

This article has been accepted for publication and undergone full peer review but has not been through the copyediting, typesetting, pagination and proofreading process which may lead to differences between this version and the Version of Record. Please cite this article as doi: 10.1111/gwmr.12547

Sulfate Land Application Enhances Biodegradation in a Petroleum Hydrocarbon Smear Zone

by Kanwartej S. Sra, Violaine Ponsin, Ravi Kolhatkar, Daniel Hunkeler, Neil R. Thomson, Eugene L. Madsen, and Timothy Buscheck

Abstract

Delivery of sulfate to petroleum hydrocarbons (PHCs) source zones and groundwater plumes is desirable to enhance biodegradation rates when treatment has become limited due to depletion of sulfate. Sulfate land application involves spreading sulfate salts on ground surface and allowing their dissolution and infiltration of sulfate into subsurface. The objectives of this pilot-scale investigation were to capture the vertical transport of sulfate beneath an application area, confirm that sulfate reduction was occurring, and explore how the added sulfate affected biodegradation of benzene and toluene. Approximately 4,000 kg of gypsum was spread over a 30 m × 30 m study area above a smear zone located ∼2 m below ground surface. Precipitation was augmented by two irrigation events. Groundwater samples, collected over 1058 days from multilevel wells and a conventional long-screened monitoring well, were analyzed for benzene, toluene, ethylbenzene and xylenes (BTEX), sulfate, bromide, dissolved inorganic carbon (DIC) and methane. Compound-specific isotope analyses (CSIA) for benzene and toluene, and isotope analyses of ^{13}C-DIC and ^{34}S-SO_4^{2-} were performed. Following application, an increase in sulfate concentration was noted in the smear zone. ^{34}S-SO_4^{2-} enrichment and ^{13}C-DIC depletion indicated that sulfate reduction and mineralization of PHCs were enhanced. CSIA results provided unequivocal evidence of anaerobic biodegradation of benzene and toluene. After 1058 days when sulfate was depleted, methane concentrations were about three times greater than baseline conditions suggesting syntrophic benefit of the

delivered sulfate. Observations from this investigation support the viability of sulfate land application to enhance biodegradation rates in shallow PHC smear zones.

Introduction

The persistence of petroleum hydrocarbons (PHCs), including specific aromatic compounds such as benzene, toluene, ethylbenzene, and xylenes (BTEX) in groundwater, is well-documented (Wiedemeier et al., 1999; Meckenstock and Mouttaki, 2011; Meckenstock et al., 2015; Prosser et al., 2016; Kolhatkar and Schnobrich, 2017; Fayemiwo et al., 2017; Buscheck et al., 2019). BTEX concentrations in groundwater naturally attenuate due to biodegradation (Wei et al. 2018) and also due to other processes, such as dilution, dispersion, sorption and volatilization (USEPA, 2012). A sustained decrease of BTEX concentrations in groundwater over time can be limited at some sites due to the lack of soluble electron acceptors (Meckenstock et al., 2015; Kolhatkar and Schnobrich, 2017). Due to these limitations, it may take decades for BTEX concentrations to reach site clean-up objectives. Along with oxygen, nitrate and ferric iron, sulfate is the most commonly depleted electron acceptor in PHC plumes and areas of residual non-aqueous phase liquid (NAPL) (USEPA, 2007; Kolhatkar and Schnobrich, 2017; Wei et al., 2018). Sulfate is a more desirable electron acceptor for delivery into PHC-impacted areas due to several important characteristics (Anderson and Lovely, 2000; Cunningham et al., 2001; Kolhatkar and Schnobrich, 2017; Wei et al., 2018):

- higher solubility, which enables delivery of a significantly higher mass load to groundwater (than ferric iron or oxygen),
- higher persistence (than oxygen) and lower non-target demand (than oxygen or nitrate),
- higher (secondary) maximum concentration level (than nitrate),

- higher capacity to accept electrons per unit weight, and
- low potential for biofouling or clogging (than oxygen or ferric iron).

In addition to the above, most PHC sites are already anaerobic (due to rapid depletion of dissolved oxygen in the presence of PHCs) and conducive to biodegradation under sulfate-reducing conditions (Foght, 2008; Meckenstock and Mouttaki, 2011; Kolhatkar and Schnobrich, 2017).

At sites where sulfate is depleted, PHC source mass typically undergoes natural bulk hydrocarbon depletion (i.e., natural source zone depletion or NSZD). The process of methanogenesis (CO_2 reduction, acetate fermentation) is an important contributor to overall NSZD, but also can be an important control on the rate of NSZD (Garg et al. 2017) due to several rate-limiting processes affecting methanogenesis. These may include unfavorable thermodynamics, less robust or minimal syntrophic populations to facilitate the initial breakdown of PHCs, and build-up of intermediates such as acetate and H_2 that could potentially inhibit BTEX biodegradation (Vogt et al., 2011; Gieg et al., 2014; Wilson et al., 2016; Garg et al. 2017). Parisi et al. (2009) reported biodegradation of non-target PHCs (e.g., alkanes such as heptane, octane, nonane, and alkylated aromatics such as 1-ethyl-3-methylbenzene) in a contaminated aquifer while target PHCs including benzene were not biodegraded. Toth et al. (2021) reported a 2 to 4 times decrease in benzene degradation under sulfate reducing or methanogenic conditions in the presence of other co-contaminants (i.e., TEX). Sulfate addition can stimulate sulfate reducing bacteria that can directly metabolize acetate and H_2 thereby preventing their buildup and making the initial breakdown of PHC (particularly benzene) thermodynamically feasible and consequently driving the syntrophic process (Vogt et al. 2011, Gieg et al., 2014). Irianni-Renno et al. (2015) suggested that PHC biodegradation

was mediated by syntrophic fermenters and methanogens in a highly contaminated smear zone and demonstrated sulfate reduction and methanogenesis contributing to hydrocarbon biodegradation in the underlying saturated zone. Siegert et al. (2011) demonstrated significant increase in hexadecane-dependent methanogenesis in the presence of increasing sulfate concentrations up to 480 mg/L in laboratory microcosms using sediment from two brackish water locations. Sulfate reducers were proposed to enrich the crucial syntrophic microbial ecosystem that is responsible for the breakdown of complex PHCs, including benzene, and their intermediates (Gieg et al., 2014). The potential for sulfate reducers to enrich the syntrophic ecosystem provides an avenue to improve the overall rate of methanogenesis and bulk hydrocarbon depletion even after sulfate is no longer available.

Delivery of amendments such as sulfate is generally limited by geology, mass load requirements, and rapid consumption (Buscheck et al., 2019). Sulfate land application can deliver sulfate over a plume footprint, and can potentially overcome mass delivery limitations, using widespread, uniform and convenient solid chemical application over large, impacted areas. Kolhatkar and Schnobrich (2017) used gypsum and Epsom land application over 13 acres (52,610 m^2) to deliver sulfate into a predominantly benzene-rich groundwater plume (benzene concentrations ranged between 800 and 4,400 µg/L, and TEX concentrations ranged between <5 µg/L and 60 µg/L) that resulted in a three-fold increase in benzene attenuation rates. Wei et al. 2018 demonstrated enhanced biodegradation of benzene, toluene and *o*-xylene downgradient of a small, dissolved sulfate infiltration pond overlying an emplaced PHC source zone. However, the spatial scale of Wei et al. (2018) study was limited, and Kolhatkar and Schnobrich (2017) did not provide insight into the transport of sulfate and was limited in its description of interactions between sulfate and PHCs (i.e., production of dissolved inorganic carbon, sulfate reduction). In addition, data in Kolhatkar and Schnobrich (2017)

primarily focused on the changes in the dissolved phase benzene concentrations (given the relatively low concentrations of TEX in groundwater) in long-screen monitoring wells. While useful, these studies also highlighted the need for a better understanding of the transport of sulfate through the vadose zone and the ability to enhance treatment of PHCs, including BTEX, in more complex settings such as a residual light NAPL (LNAPL) source zone.

For most land application methods, it can be challenging to demonstrate that the applied amendments are being consumed and enhanced degradation of the target compounds is occurring. Recent advances in diagnostic tools (DTs) including compound-specific isotope analysis (CSIA), and molecular biological tools (MBTs) or biomarkers for specific PHCs have improved the ability to assess performance of remedial systems involving biodegradation of PHCs (Griebler et al., 2004; Fischer et al., 2008; Knöller et al., 2008; Batlle-Aguilar et al., 2009; Fischer et al., 2009; Morasch et al., 2011; Braeckevelt et al., 2012; Feisthauer et al., 2012; Thullner et al., 2012; Ponsin et al., 2015; Torrentó et al., 2017; Bouchard et al., 2018a; Shayan et al., 2018; Solano et al., 2018; Wei et al., 2018; Wanner et al. 2019). The use of biomarkers relies on the detection and quantification of "signature" metabolites, which are specific to a transformation pathway for a given compound, and/or the detection of mRNA encoding for enzymes involved in the associated biodegradation pathways (Bombach et al., 2010; Laban et al., 2010; Liu et al., 2011;). Metabolites can be specific to a compound and a redox condition (Weelink et al., 2010; El-Naas et al., 2014; Gibson and Parales, 2000). The detection of specific mRNA transcripts in high abundance is a strong indicator of the success of a remediation strategy that aims to stimulate specific microorganisms and thereby enhance biodegradation (Toth et al., 2021). Stable isotope analysis can also be applied to electron acceptors and by-products to provide unequivocal evidence for i) the consumption of electron acceptors if an enrichment in heavier isotope is observed (e.g., $^{34}S\text{-}SO_4^{2-}$ in Schroth et al., 2001; Knöller et al.,

2006; Feisthauer et al., 2012; Buscheck et al., 2019), and ii) the mineralization of PHCs if depletion of ^{13}C in dissolved inorganic carbon (DIC) is observed (Bolliger et al., 1999; Hunkeler et al., 1999; Buscheck et al., 2019). Following infiltration of dissolved sulfate, Wei et al. (2018) demonstrated an associated evolution of sulfate concentration, enrichment of $^{34}S\text{-}SO_4^{2-}$ and depletion of ^{13}C-DIC, and enrichment of ^{13}C and / or ^{2}H in BTX which indicated delivery of sulfate, reduction of applied sulfate, mineralization of PHCs, and biodegradation of target PHCs, respectively. Quantification of biomarkers such as metabolites (i.e., benzylsuccinate and 2-methylbenzylsuccinate) were indicative of anaerobic biodegradation of toluene and xylenes. Genes encoding for enzymes included 1) anaerobic benzene carboxylase (*abcA*, mRNA that is active in anaerobic benzene metabolism), 2) benzylsuccinate synthase (*bssA-SRB*, mRNA active in anaerobic toluene metabolism under sulfate-reducing conditions), and 3) dissimilatory sulfate reductase (*dsrB*, mRNA linked to the reduction of sulfate in anaerobic conditions) and provided additional support that toluene and o-xylene were undergoing anaerobic biodegradation under sulfate-reducing conditions which were absent prior to sulfate delivery. Similarly, Shayan et al. (2018) used a combination of CSIA and biomarker tools during a controlled injection of persulfate into a BTX plume to identify dominant mass removal process within the treatment zone.

The focus of this study was to understand the efficacy and performance of sulfate land application at a PHC-impacted site. The selected land application area was situated above a PHC residual source zone in a predominantly silty clay soil overlying a sandy zone with PHC impacts in both soil and groundwater, including significant concentrations of BTEX. The objectives were: 1) to understand the vertical transport of sulfate, 2) to establish sulfate reduction, and 3) to investigate the impact of sulfate addition on BTEX biodegradation and

methanogenesis. Understanding these relevant processes and their efficacy will help inform and improve the design of sulfate land application approaches.

Methods

Study area description

This investigation focused on a 900 m^2 plot of land within a 400 hectare (990 acre) former refinery site located in the US Midwest with relatively permeable geology and shallow hydrocarbon impacts (**Figure 1**). Local stratigraphy consists of a thin layer of topsoil underlain by a silty clay, clay and clayey sand unit extending from 0.6 to 2.9 m below ground surface (bgs), followed by poorly graded sand to a depth of ~6 m bgs. This sandy zone is underlain by basal clay of variable thickness (4 to 10 m). This location was part of a former aboveground tank farm that was used to store refined PHC products but is now free of surface infrastructure and supports an intermittent grass cover. Based on historical data, the groundwater table has been observed to fluctuate within the finer-grained unit from 0.8 and 2.7 m bgs. The groundwater flow direction in the sandy zone beneath the study plot is southeasterly with an estimated velocity of about 0.4 m/day based on single-well point-dilution tests.

Four boreholes were advanced to a depth of 4.5 m bgs using direct push technology (Geoprobe® 6620T) within the study area (**Figure 1a**). Soil cores were visually logged to qualitatively assess stratigraphy and the presence of PHCs, and photoionization detector (PID) readings were taken every 0.6 m. PHC impacts were identified as being vertically distributed (i.e., a smear zone) largely within the range of groundwater table fluctuations (PID reading up to 1,000 ppm). These observed PHC impacts were in contact with underlying groundwater and presumably contribute to the existing shallow groundwater plume consisting primarily of BTEX. Elevated concentrations of BTEX (>1,000 µg/L) were measured in the samples collected

from existing long-screened monitoring well MW9 (5-cm internal diameter Schedule 40 PVC screened from 1.52 to 4.57 m bgs) located within the study area. At shallower depths of <1 m bgs, the soil was almost completely devoid of BTEX probably due to aerobic biodegradation or volatilization. Low concentrations of other non-BTEX compounds may have been present at these depths as indicated by the PID readings (**Figure 2a**).

To support this study, the four borehole locations were completed with multilevel (ML) groundwater monitoring points (MPs) (**Figure 1b**). Each borehole location (MP1 to MP4) was equipped with four nested MLs (Schedule 40 PVC with 2.5 cm ID) discretely screened across the following depth intervals: 1.52 to 1.67 m bgs (A depth interval), 2.44 to 2.59 m bgs (B depth interval), 3.35 to 3.50 m bgs (C depth interval), and 4.27 to 4.42 bgs (D depth interval). Conventional monitoring well (MW8) located ∼50 m upgradient of the study area was used in this effort as a control location. A few other conventional monitoring wells in the vicinity of the study area, which were not part of this study but routinely monitored for site management purposes, were used for comparison and evaluation of dissolved methane within the study area.

Sulfate Application and Irrigation Events

Sulfate land application was carried out by applying granular agricultural gypsum ($CaSO_4 \cdot 2H_2O$, USA Gypsum, PA, USA) at the rate of 4.4 kg/m^2 along with (calcium) bromide ($CaBr_2$, TETRA Technologies, TN, USA) at a rate of 0.055 kg/m^2 on Day 0. Bromide was included as a conservative tracer to track the fate of the infiltrating solution. The gypsum application rate was chosen to be consistent with typical gypsum loadings often employed in agronomy (OSU, 2011). A total of 4,080 kg of gypsum and 50 kg of calcium bromide were applied. Following application of the salts, the top 5 to 7 cm of the top-soil layer was gently tilled using

agricultural equipment, and a 30-cm high berm was created around the study area to allow for focussed infiltration, and to minimize loss of irrigation water or precipitation runoff. To assist with initial sulfate transport (dissolution and infiltration), the study area was flooded with sufficient water from a local surface water source to create a ponded water depth of ∼5 cm (Irrigation Event-1). Based on the volume of water used in this event (∼45 m^3) and the solubility of the salts applied, it was expected that residual salt mass would be present in the top-soil layer after all the irrigation water had infiltrated. Following Irrigation Event-1, precipitation (rainfall and snow) events were responsible to dissolve this residual salt mass and drive the dissolved sulfate and bromide deeper into the subsurface.

Results from a coring event conducted on Day 470 indicated that residual mass of sulfate (∼45%) and bromide (∼39%) was present in the vadose zone. These results suggested that precipitation alone was insufficient to transport the salt mass through the finer-grained unit and into the sandy zone. As a result, Irrigation Event-2 from Day 644 to Day 756 was undertaken to mobilize the retained sulfate and bromide in the vadose zone. A local surface water source was used weekly to flood the study area to a ponded water depth of ∼5 cm (total volume of ∼720 m^3).

Groundwater Sampling and Analyses

Groundwater sampling was undertaken to capture the spatial and temporal changes in the concentrations of BTEX, sulfate, DIC, and methane in groundwater. Since concentration changes in these constituents could be unrelated to reactive processes, diagnostic tools (CSIA, biomarkers, isotope analysis) were used to obtain unequivocal evidence for sulfate reduction, stimulation of target PHC biodegradation and for complete mineralization of PHCs. Prior to sulfate land application on Day 0, baseline groundwater samples were collected from the MPs

and MWs using a low-flow sampling approach with a peristaltic pump (Geotech, Model Geopump II). Temperature, pH, oxidation-reduction potential, conductivity, turbidity and dissolved oxygen were monitored using a flow-through cell and a multiparameter water quality meter (Horiba U-53). Six post-sulfate application groundwater sampling events at the MPs and MWs were completed over a period of 1058 days (i.e., on Day 309, Day 470, Day 644, Day 700, Day 756 and Day 1058; see **Supporting Information Table SI-1** for a detailed sampling and analyses plan). Groundwater sampling primarily focused on the B and C depth interval MPs (the A depth interval was dry), and one conventional monitoring well MW9. Samples were collected for the analysis of sulfate, bromide, DIC, BTEX, dissolved methane and CSIA on benzene and toluene, isotope analysis on sulfate and DIC, and biomarkers (except on Day 309 and Day 700).

Analyses of ions, BTEX, DIC, and dissolved CH_4 were performed by Eurofins TestAmerica Laboratories, Inc (USA). Samples for ^{13}C-DIC and ^{34}S-SO_4^{2-} were analyzed at the University of Waterloo following procedures described in Bouchard et al. (2018b) and Shayan et al. (2018), respectively. Groundwater samples for CSIA of benzene and toluene were analyzed following the method described in Ponsin et al. (2017). For CSIA, the limit of precise isotope analysis (i.e., the limit to reach a standard deviation ≤0.2‰ for carbon and ≤5 ‰ for hydrogen), was 5 µg/L and 30 µg/L, respectively. Biomarkers (select genes and metabolites) were analyzed at Cornell University or Microbial Insights following methods described in Bouchard et al. (2018) (see **Supporting Information Table SI-1** for additional details on biomarker analysis). Biomarker data was employed where possible; however, biomarker sample collection and preservation are not routinely conducted at environmental sites and are more difficult than those for conventional groundwater analytes. Therefore, less certainty could be associated with the biomarker data results in this study. For example, an absence of detectable specific

transcripts or metabolites was not considered conclusive evidence of lack of PHC biodegradation under specific redox conditions (Parisi et al., 2009). If specific transcripts were absent, it was possible that PHC biodegradation was still occurring but either the indigenous microorganisms were utilizing a pathway relying upon as-yet uncharacterized genes or that the assay was not sufficiently sensitive to detect ambient low levels of a transcript.

Soil Sampling and Analyses

To estimate the remaining mass of sulfate in the vadose zone and to determine evidence of sulfate reduction, a soil sampling event was conducted on Day 470. Cores were advanced using direct push technology close to MP2, MP3, MW8, and MW9 (see locations on **Figure 1a**). Soil cores were advanced up to a depth of ~2.7 m bgs, and sub-samples were analyzed for sulfate, bromide, BTEX, sulfide, total iron, Fe(II), and $^{34}S\text{-}SO_4^{2-}$. Sub-sample handling and analyses details are provided in the **Supporting Information Section SI-2**.

Results and discussion

Baseline Conditions and Conceptual Model

Soil PID measurements collected during the initial soil coring event at the MP locations, and concentrations of BTEX and sulfate in groundwater at the B, C and D depth intervals are shown on **Figure 2** (the A depth interval was dry). PID readings >1,000 ppm are indicative of significant PHC impacts (Otton and Zielinski 2000), and thus the majority of PHC mass appears to be located between 1.0 and 3.5 m bgs (**Figure 2a**). This observation is consistent with PHC profiles from historic site investigations (data not shown), and BTEX results from the Day 470 soil coring event. Specifically, total BTEX concentrations in soil samples collected from <2 m bgs on Day 470 range from below detection (0.5 mg/kg for individual BTEX compounds) to 1,100

mg/kg, while higher total BTEX concentrations (760 to 6,800 mg/kg) were detected between 2.0 and 2.7 m bgs (encompassing the B depth interval) indicative of a smear zone (**Figure 5**). Depth to water table fluctuated between 1.6 and 2.6 m bgs during this study and is within the range of groundwater fluctuations noted historically. **Figure 2b** shows a decrease in benzene groundwater concentrations from the B to C and D depth intervals; 9,800 to 16,000 µg/L benzene at the B depth interval, 0.5 to 6 µg/L benzene at the C depth interval, and 0.3 to 13 µg/L benzene at the D depth interval. TEX concentrations decreased from the B depth interval (between 12,000 and 54,300 µg/L) to the C depth interval (between 62 and 714 µg/L) and to the D depth interval (between 3 and 291 µg/L). In contrast, sulfate concentrations were low (<19 mg/L) at the B and C depth intervals while elevated (30 to 100 mg/L) at the D depth interval likely indicative of near-ambient sulfate conditions in the sandy zone (**Figure 2c**). At the long-screened monitoring well MW9, moderate benzene (250 µg/L) and TEX concentrations (775 µg/L) and a low sulfate concentration (2 mg/L) were noted, representing a blend of groundwater from vertical zones adjacent to the well screen. The "average" concentrations of BTEX, sulfate and DIC in this blend are dependent upon profiles of concentration and flux of groundwater entering the well screen. Despite this averaging effect for a long-screened monitoring well, results for the baseline conditions are still consistent with the inverse relationship between BTEX and sulfate (**Figure SI-1**). BTEX concentrations, particularly at shallow depths (i.e., B depth interval) are indicative of the presence of residual LNAPL, which continuously supplies BTEX into the aqueous phase through dissolution and thus maintains elevated BTEX concentrations. The noted decrease in BTEX concentrations with depth is consistent with a historical near-surface release of LNAPL and the existence of a smear zone (USEPA, 1995). Mass discharge (of PHCs and applied salts) from finer-grained soils at shallow depths into the sandy zone may also be diluted by ambient groundwater movement

in this zone resulting in significant contrasts between concentration profiles at B and C depth intervals. The contrasting concentration profiles between B and C depth intervals could also result from sorption and matrix diffusion of PHCs within the finer-grained soils that can limit rapid transport to the underlying sandy zone. Sulfate concentration for D depth interval suggests that sulfate may be more readily recharged or available within the sandy zone to contribute to rapid depletion of PHCs. Overall, the depleted sulfate concentrations in the presence of BTEX suggest ongoing sulfate reduction with sulfate as a limiting electron acceptor (Kolhatkar and Schnobrich, 2017) and support the hypothesis that sulfate addition could enhance biodegradation of BTEX and other PHCs.

Figure 3 conceptually illustrates the anticipated behavior of the land application of sulfate in this study to enhance sulfate reduction within the smear zone and in the underlying saturated zone. Findings from historical site-wide investigations (not shown) and data collected to support this study indicate that within the study area a spatially extensive BTEX plume exists in the sandy zone (2.3 to 6.0 m bgs), and that residual NAPL is present (~2.0 to 2.7 m bgs) near the top of the sandy zone and into the overlying finer-grained material due to the historical water table fluctuations (0.8 to 2.7 m bgs). During the timeframe of this study, the water table fluctuated between 1.6 and 2.6 m bgs (**Supporting Information Figure SI-2**) resulting in transitions from aerobic to anaerobic conditions. Under high water table conditions, dissolved oxygen and other soluble electron acceptors including sulfate (if present) would be quickly depleted in the residual NAPL zone, and then the system would shift to methanogenesis. Vertically driven by irrigation and natural infiltration processes due to rainfall or snowmelt, the applied sulfate on the land surface is expected to dissolve and migrate into and through the NAPL smear zone. The presence of elevated sulfate within the smear zone should promote favorable conditions for the growth of indigenous sulfate-reducing bacteria (SRB)

communities. Enhanced sulfate reduction should lead to a decrease in the concentration of some BTEX and sulfate in groundwater, and an increase in the groundwater concentration of DIC and sulfide (**Figure 3**) although geochemistry (e.g., carbonate equilibrium, Fe(II) presence, pH changes) will control the evolution of carbonic species and precipitation of sulfide.

Due to the presence of residual NAPL, elevated BTEX concentrations, mixing of infiltrating water with ambient groundwater (particularly in the sandy zone), and interaction of applied sulfate with PHCs, concentration changes for either sulfate, DIC or BTEX in groundwater alone were not expected to be sufficient to confirm the anticipated shift to sulfate reducing conditions. Since dissolution from the residual NAPL in the smear zone was also anticipated to mask the likely enrichment in ^{13}C and ^{2}H of BTEX due to biodegradation, monitoring changes in $^{34}S\text{-}SO_4^{2-}$, and ^{13}C-DIC would be important as indicators of sulfate reduction leading to mineralization of PHCs. Due to averaging effect for a long-screened monitoring well at MW9, the concentration and isotopic changes at MW9 were expected to be moderate in comparison to discrete depth intervals.

Enrichment of $^{34}S\text{-}SO_4^{2-}$ in both soil and groundwater samples was expected to show that sulfate was reduced following land application. This sulfate reduction can be linked to PHC biodegradation through use of ^{13}C-DIC, which is expected to be depleted in groundwater while PHC mineralization is occurring under sulfate reducing conditions (Landmeyer et al., 1996, Bouchard et al., 2018a, Wei et al., 2018). The remaining BTEX in groundwater should be enriched in ^{13}C and ^{2}H at depths where groundwater is not directly in contact with residual NAPL (Bouchard et al. 2018a). Current knowledge of microorganisms capable of biodegrading benzene under anoxic conditions is still incomplete and microbial pathways for anaerobic biodegradation of benzene were not fully elucidated at the time of this study (Meckenstock et al. 2016; Toth et al., 2021). As a result, the database of biomarkers for anaerobic benzene

biodegradation is rather limited compared to toluene. Biomarker evidence for increased sulfate reduction was expected to include an increase in $bssA_{srb}$ transcripts, which are associated with biodegradation of one or more of toluene, ethylbenzene and xylenes (TEX) under sulfate-reducing conditions. Biomarker evidence for increased anaerobic biodegradation of benzene was expected to include *abcA* transcripts (Bouchard et al. 2018a).

Temporal Evolution of Sulfate and BTEX

Following sulfate application on Day 0, both bromide and sulfate concentrations in samples collected from the B depth interval and MW9 were elevated (**Figure 4**) by Day 309 compared to baseline concentrations confirming that the applied sulfate and bromide salts had dissolved into water (precipitation and / or irrigation, **Figure 4a**) and infiltrated. As expected, the highest concentrations of sulfate and bromide were detected at the shallowest monitoring points (i.e., the B depth interval as compared to the C and D depth intervals). For the B depth interval, the average bromide concentration increased to 26 mg/L by Day 309 and then declined to 10 mg/L by Day 644 before undergoing a minor increase (to 19 mg/L) on Day 700 in response to Irrigation Event-2. In contrast, the bromide concentration at the C and D depth intervals showed no increase (0.2 to 0.5 mg/L at the C depth interval, and 0.1 to 0.3 mg/L at the D depth interval) except for a spike at the C depth interval on Day 756 to 2 mg/L likely in response to Irrigation Event-2. Average sulfate concentration (**Figure 4b**) at the B depth interval increased to 44 mg/L by Day 309 and then decreased to baseline conditions (<10 mg/L) by Day 700. Sulfate concentration at B depth interval increased to 187 mg/L by Day 756 in response to Irrigation Event-2. Sulfate concentrations at the C and D depth intervals showed no significant change (0.1 to 1.4 mg/L at the C depth interval, and 27 to 59 mg/L at the D depth interval)

until an increase to 13 mg/L at the C depth interval on Day 700 in response to Irrigation Event-2. The bromide and sulfate concentration trends following Irrigation Event-2 (**Figures 4b and 4c**) suggest that bromide and sulfate retained in the vadose zone were mobilized. This remobilization also led to a notable increase in sulfate and bromide concentrations in the C depth interval as noted for Day 700 or Day 756. The greater irrigation volume ($\sim$720 m^3) during Irrigation Event-2, also potentially helped overcome the dilution effect from ambient groundwater flow in the sandy zone resulting in an increase in bromide and sulfate concentrations. Sulfate concentrations at the B depth interval on Day 1058 could not be confirmed due to a low water table. Bromide and sulfate concentrations at the C depth interval declined to baseline conditions following termination of Irrigation Event-2 likely due to decreased vertical flux of dissolved salts in addition to the dilution of infiltrating water by ambient groundwater in the sandy zone.

A comparison of the temporal profiles of bromide (assumed to be conservative) and sulfate indicates that sulfate breakthrough was relatively delayed with respect to bromide (**Figures 4b and 4c**). For example, at MW9, the peak breakthrough concentration of sulfate (Day 470) was delayed with respect to peak breakthrough concentration of bromide (Day 309). Sulfate breakthrough is expected to be delayed since it is consumed during the biodegradation of PHCs present at depths >1 m bgs. The difference in bromide and sulfate breakthrough trends at the B vs C and D depth intervals is also linked to dilution by ambient groundwater (for bromide and sulfate) and consumption (for sulfate) as the dissolved salts are transported vertically. The B depth interval MPs are screened in the fine-grained soils (**Figure 1b**) whereas the C and D depth interval MPs are screened in the sandy zone. Consequently, the horizontal groundwater flow at the C and D depth intervals is much larger than at the B depth interval and vertical flux of bromide and sulfate would be diluted at C and D depth intervals. Between

the C and D depth intervals, the C depth interval had a higher concentration of bromide but a lower concentration of sulfate. While land application was the source of bromide and, therefore had a profile indicative of downward vertical transport, the sulfate profile was complicated by the presence of ambient sulfate at the D depth interval, where background sulfate concentrations of 30 to 100 mg/L were observed. The low to non-detect concentrations of sulfate at the C depth interval suggest that sulfate was consumed in zones shallower than the C depth interval and / or was diluted by ambient groundwater deeper than the B depth interval.

Bromide concentration in MW9 increased to 38 mg/L by Day 309 followed by a steady decrease to baseline levels by Day 756 with no apparent impact of Irrigation Event-2. Sulfate concentration in MW9 demonstrated a substantial and sustained increase from Day 309 until Day 756 after which sulfate concentrations declined to near-baseline conditions. This sustained increase at MW9 could be due to the long-screened interval which can source sulfate-laden groundwater from a thicker saturated zone than that is possible for short, discrete multilevels. The concentration of sulfate and bromide at the B depth interval, although elevated from the baseline conditions, were variable across the four monitoring locations (**Figures 4b and 4c**) likely due to physical and chemical heterogeneities. The local stratigraphy shallower than 2.9 m bgs includes variable layers of silty clay, clay and clayey sand, which influence both the infiltration of water laden with sulfate and bromide and the distribution of PHCs (and any consumption of sulfate) resulting in non-uniform breakthrough.

BTEX concentrations at the B depth interval remained elevated with average concentrations across all B depth interval MPs ranging from 23,000 to 42,000 µg/L (see **Figure SI-3**). Groundwater in and around the B depth interval is in contact with residual NAPL. Therefore,

persistent dissolution of PHCs such as BTEX would mask any concentration decreases due to natural or induced attenuation processes. As such, dependence solely on observing discernable change in groundwater concentrations of BTEX under such conditions is an unreliable approach to assess treatment performance.At the C depth interval, a steady decrease of total BTEX concentration from 250 to 70 µg/L was observed between Day 0 and Day 644, followed by an increase to 8,900 µg/L in response to Irrigation Event-2. This sharp increase was likely due to the aqueous BTEX mass migrating downward by the sustained irrigation between Day 666 to Day 756. At MW9, total BTEX concentrations ranged between 1,000 and 3,000 µg/L, and benzene concentrations ranged between 250 and 1,900 µg/L.

Assessment of Sulfate Reduction

Soil Core Data

Bromide and sulfate bulk soil concentrations from Day 470 indicate that both constituents (maximum of 7.9 mg/kg for bromide and 613 mg/kg for sulfate at a depth of ∼0.8 m bgs) were significantly (>10 times) higher compared to those at the soil core location near MW8 (generally non-detect for bromide and a maximum of 55 mg/kg sulfate at a depth of ∼1 m bgs) upgradient of the study area (**Figures 5a and 5b**). These results further confirm that this land application strategy supported by precipitation and irrigation was able to vertically distribute land applied salts.

Since bromide is conservative, it was relatively elevated (averaging between 1.0 and 4.7 mg/kg) across the entire soil core depth interval (**Figure 5a**). Sulfate was generally higher (averaging between 285 to 420 mg/kg) to a depth ∼1 m bgs but then decreased 10-fold by ∼2 m bgs (**Figure 5b**). Bulk BTEX soil concentrations were non-detect (<0.1 mg/kg) at depths less than ∼1 m bgs both within the study area and near MW8. BTEX was relatively elevated deeper

than 1 m bgs, particularly in the soil core collected near MW8 (166 to 223 mg/kg), and within the study area at around 2 m bgs (**Figure 5c**). Low BTEX concentrations at shallow depths (<1 m bgs) are likely indicative of influence of atmospheric oxygen-induced aerobic biodegradation, and possible loss through volatilization and dissolution over time. The depleted sulfate trend with respect to bromide at depths >1 m bgs is expected since the relative abundance of PHCs (including BTEX) below that depth would result in sulfate consumption during biodegradation (**Figure 2 and Figure 5c**) and bromide being a conservative tracer would not be affected.

Sulfide was detected in deeper horizons (e.g., ≥1.2 m bgs, **Figure 5d**) which indicates that sulfate reduction likely occurred where PHCs were relatively abundant. Corresponding to the sulfide profile, the ratio of ferrous iron (Fe^{2+}) to ferric iron (Fe^{3+}), a measure of the extent of ferrous sulfide precipitation (**Figure 5e**) was ∼2 orders of magnitude higher. The predominance of ferrous iron at a depth ≥1.2 m bgs as compared to shallower depths suggests that ferrous sulfide precipitation had occurred. Lack of sulfide and ferrous iron at shallower depths (≤1 m bgs) may be indicative of oxic conditions where sulfide was oxidized to sulfate by the oxygen-rich precipitation water or irrigation water (Ulrich et al. 2003; Knöller et al., 2008), oxygen influence during water table fluctuation (Teramoto et al., 2020), or lack of sulfate reduction at shallow depths where PHCs were less abundant. The lower Fe^{2+}/Fe^{3+} ratio at depths shallower than ≤1 m bgs also indicates the presence of oxic conditions.

Overall, these observations provide evidence that sulfate reduction was occurring in the presence of PHCs in the vadose zone as sulfate-rich water infiltrated through this zone. It is hypothesized that concomitant oxidation of PHCs in the vadose zone was also occurring as sulfate underwent reduction. This implies that sulfate land application may be applicable as

a remediation strategy for targeting treatment of vadose zone PHC impacts. This also implies that as sulfate is being utilized (reduced) in the vadose zone, less of it would be transported into the saturated zone where it is expected to interact with PHCs and where typical monitoring of sulfate breakthrough or of target PHCs concentration decrease occurs.

Diagnostic Tools

Reduction of sulfate is further confirmed by the stable isotope trends for sulfur in sulfate in both the soil cores and in the groundwater (**Figures 5b and 6**). **Figure 5b** illustrates that ^{34}S-SO_4^{2-} in soil sub-samples collected on Day 470 was enriched (4.1 to 48.1‰) in comparison to the source gypsum ^{34}S-SO_4^{2-} (3.2‰). An inverse trend between bulk soil sulfate concentration and ^{34}S-SO_4^{2-} demonstrates that the lower sulfate concentrations were, in part, a consequence of sulfate reduction. The heavier isotope was more enriched at depths ≥1.2 m bgs with the highest enrichment (48.1‰) observed at the deepest sub-sample location at 1.9 m bgs in the smear zone. This trend is consistent with the observations of sulfide and Fe^{2+} discussed above and provides confirmation that sulfate reduction was occurring where significant PHC concentrations (e.g., BTEX >100 mg/kg) were present (**Figure 5c**).

Figure 6 shows the temporal profiles of SO_4^{2-}, $\delta^{34}S$-SO_4^{2-}, DIC and $\delta^{13}C$-DIC for the B and C depth intervals, and for MW9. Enrichment of ^{34}S-SO_4^{2-}, and therefore sulfate reduction (Knöller et al., 2008; Feisthauer et al., 2012), is evident at all locations both in comparison to the baseline conditions (-4.8‰) and to the source gypsum ^{34}S-SO_4^{2-} (3.2‰). A greater degree of sulfate reduction, and correspondingly higher average ^{34}S-SO_4^{2-} enrichment, was observed at the B depth interval (28.4 to 43.3‰) compared to the C depth interval (up to 26.2‰ on Day 700) and MW9 (up to 15.5‰ on Day 644). At the B depth interval, ^{34}S-SO_4^{2-} significantly increased from a baseline average value of -4.8‰ to 43.3‰ on Day 644 before decreasing to

an average value of 29.0‰ on Day 756. This decrease between Day 644 and Day 756 was likely associated with Irrigation Event-2 which led to a sharp increase in sulfate concentrations at the B depth interval as a result of the migration of relatively unreduced sulfate from shallower depths to the B depth interval, thereby partially masking the enrichment of $^{34}S\text{-}SO_4^{2-}$. Despite the potential masking effect, $^{34}S\text{-}SO_4^{2-}$ in groundwater at the B depth interval continued to remain strongly enriched, indicating sustained sulfate reduction. Sulfate concentrations at the C depth interval were generally too low (<5 mg/L) for isotope quantification and therefore, only two measurements of $^{34}S\text{-}SO_4^{2-}$ could be obtained. These data indicate that the $^{34}S\text{-}SO_4^{2-}$ during Irrigation Event-2 was much more enriched than the source gypsum signature or the B depth interval baseline signature. This enrichment of $^{34}S\text{-}SO_4^{2-}$ at the C depth interval is attributed to a combination of sulfate reduction occurring both above and within the C depth interval . Similarly, strong enrichment in $^{34}S\text{-}SO_4^{2-}$ (between 9.8 and 16.5‰) at MW9 indicated that significant sulfate reduction was occurring. Although the $^{34}S\text{-}SO_4^{2-}$values from MW9 were enriched compared to the signature of applied gypsum, the enrichment was lower compared to the values from the B and C depth intervals due to blending of groundwater with unenriched or ambient sulfate (e.g., from D depth interval).

Biodegradation of PHCs

Mineralization of PHCs

Baseline $\delta^{13}C$-DIC values ranged from -4.2 to 6.3‰ at the B and C depth intervals, and at MW9 (**Figure 6**). These relatively enriched $\delta^{13}C$-DIC values (compared to -10.2‰ to -1.4‰ for D depth interval representing ambient conditions) are likely a result of ongoing methanogenesis that produces ^{13}C-enriched CO_2 (Conrad et al. 1997; Landmeyer et al. 1996; Teramoto et al.,

2020). Landmeyer et al. (1996) reported δ^{13}C-DIC values from -11.1 to 4.5‰ where methanogenesis was confirmed.

DIC concentrations following sulfate application and Irrigation Event-1 at the B depth interval steadily increased from an average of 86 mg/L to 123 mg/L until Day 644 while ^{13}C-DIC became depleted from an average of 0.3‰ to -18.8‰. DIC is a direct indicator of dissolved carbonic species generated through complete mineralization of PHCs. DIC produced by complete mineralization of PHCs via non-methanogenic process tends to have a similar isotopic composition (i.e., in the range of -25 to -35‰) to the PHCs that are biodegraded (Aggarwal et al. 1997; Bolliger et al. 1999). The increase in DIC concentrations suggests that PHC biodegradation was occurring and was proceeding to complete mineralization (or production of CO_2) and a depletion in ^{13}C-DIC indicates that biodegradation was mediated by a non-methanogenic process such as sulfate reduction (Landmeyer et al., 1996). At the C depth interval, a similar trend toward more depleted ^{13}C-DIC was noted between Day 0 and Day 644 (from 3.5‰ to -7.4‰), although DIC concentrations showed only a minor increase possibly due to carbonate buffering. During Irrigation Event-2, a further shift toward more depleted ^{13}C-DIC at the B and C depth intervals highlights the impact of sulfate-reduction on PHC biodegradation. Landmeyer et al. (1996) reported δ^{13}C-DIC values less than -12.7‰ in shallow zones which received sulfate from surface recharge. In general, a greater increase in DIC concentrations and a greater depletion in ^{13}C--DIC was noted at the B depth interval (maximum DIC of 243 mg/L on Day 644 and minimum ^{13}C-DIC of -23.7‰ on Day 756) than at the C depth interval (maximum DIC of 121 mg/L on Day 644 and minimum ^{13}C-DIC of -13.4‰ on Day 756) indicating a greater sulfate interaction with PHCs and a higher degree of complete mineralization at the B depth interval compared to the C depth interval. This observation is supported by the larger enrichment in ^{34}S-SO_4^{2-} at the B depth interval as compared to C depth

interval. At MW9, DIC concentrations fluctuated between 65 and 120 mg/L whereas ^{13}C-DIC was generally depleted from baseline conditions (4.5‰) to between -11.6‰ (on Day 1058) and -16.7‰ (on Day 470). Enrichment in ^{13}C-DIC from Day 756 (-16.3‰) to Day 1058 (-11.5‰) corresponded with a decrease of sulfate from 270 to 4.6 mg/L and is likely due to ensuing methanogenic conditions (Landmeyer et al., 1996). Overall, the behavior of DIC and δ^{13}C-DIC confirmed that sulfate addition stimulated sulfate-reducing bacteria leading to breakdown and mineralization of PHCs (Gieg et al., 2014).

Biodegradation of Benzene and Toluene

CSIA – Dual element isotope plots

The carbon and hydrogen stable isotope data for benzene and toluene in groundwater from the MPs and MW9 are shown on **Figure 7**. These are plotted as $\Delta\delta^2$H vs $\Delta\delta^{13}$C representing differences between the measured δ^{13}C and δ^2H values and the corresponding average isotopic values for carbon and hydrogen in the residual NAPL *source*. The isotopic values of the source of benzene and toluene were unknown and hence were estimated (see **Section SI-3 for details**). For benzene, the estimated source isotopic values were -28.1 ± 0.6 ‰ for δ^{13}C (n = 21) and -92.0 ± 11.8 ‰ for δ^2H (n = 17). For toluene, the estimated source isotopic values were -27.1 ± 0.4 ‰ for δ^{13}C (n = 11) and -73.8 ± 4.6 ‰ for δ^2H (n = 9) (**Figure SI-4**). The expected range of $\Delta\delta^2$H vs. $\Delta\delta^{13}$C values associated with benzene and toluene biodegradation under anaerobic conditions are displayed as shaded zones on the panels in **Figure 7**. These ranges were established based on the lowest (17 for benzene and 20 for toluene) and highest (42.5 for benzene and 41 for toluene) lambda (Λ) values from the literature (see Mancini et al., 2008; USEPA, 2008; Aelion et al., 2009 and Bouchard et al., 2018a for a compilation of

available carbon-hydrogen isotope slopes associated with different transformation processes). The measured carbon and hydrogen stable isotope data ($\delta^{13}C$ and $\delta^{2}H$) for benzene and toluene for the B and C depth intervals are summarized in **Tables SI-2 and SI-3**, respectively.

No isotopic enrichment was observed for benzene in any of the samples collected (benzene ranging from 860 to 19,000 µg/L) from the B depth interval **(Figure 7a)** suggesting that either benzene had not degraded at these locations or that biodegradation, and corresponding isotopic enrichment, was occurring but the signature was masked by ongoing benzene dissolution from the residual LNAPL. On the other hand, significant carbon and hydrogen isotopic enrichment relative to the estimated source signature was observed for toluene at MP1B and MP2B for all sampling events (maximum enrichment of +3.5 ‰ for carbon and +109.8 ‰ for hydrogen at MP2B at Day 309, see Figure SI-5). This isotopic enrichment occurred within the zone characteristic of anaerobic biodegradation of toluene **(Figure 7b)** suggesting active biodegradation at the B depth interval at these two locations. No significant isotopic enrichment was observed for toluene at MP3B and MP4B where concentrations were one order of magnitude higher (18,000 to 39,000 µg/L) than those at MP1B and MP2B (570 to 7,850 µg/L). This lack of toluene enrichment at MP3B and MP4B was likely due to ongoing dissolution from residual LNAPL, resulting in higher toluene concentrations, which would likely mask the isotopic signature even if toluene biodegradation was occurring.

Benzene (concentration ranging from 8.6 to 310 µg/L) in all samples collected from the C depth interval (except from MP2C and MP3C on Day 700) following sulfate application showed significant isotopic enrichments in carbon and hydrogen **(Figure 7a)** providing clear evidence for benzene biodegradation. The observed hydrogen isotopic enrichment for benzene at the C depth interval was greater than the upper bound of the expected range of anaerobic

biodegradation from the literature. The carbon enrichment for benzene ranged from +0.6 ‰ (MP1C, Day 309) to +3.1 ‰ (MP2C, Day 470, see Figure SI-5), while the hydrogen enrichment ranged from +5.6 ‰ (MP3C, Day 644) to +143.6 ‰ (MP2C, Day 309, see Figure SI-5). This enrichment was present even when sulfate concentrations were negligible (<0.25 mg/L) and, therefore, suggests a possible role of syntrophic biodegradation of benzene (Vogt et al. 2011, Gieg et al., 2014). Given the low concentrations of benzene (0.6 to 6 µg/L) at Day 0, only ^{13}C could be quantified in samples from MP1C and MP4C ($\Delta\delta^{13}C$ = -0.15 ‰ for both). The similarity of the carbon isotopic signature to the source suggests that benzene in the C depth interval on Day 0 was relatively undegraded and that the isotopic enrichment for ^{13}C and ^{2}H occurred over time after sulfate land application. Benzene concentrations on Day 700 at MP2C and MP3C were 20,000 and 9,100 µg/L, respectively, suggesting that possible isotopic enrichment due to biodegradation could have been masked due to benzene dissolution from residual LNAPL. This may also be attributed to competitive inhibition of benzene biodegradation in the presence of other compounds such as toluene (Charng et al., 1993), or preferential biodegradation of PHCs other than benzene (Gieg et al., 2014; Toth et al., 2021). Parisi et al. (2009) demonstrated that benzene biodegradation was not occurring in the field or in laboratory microcosms even though a high rate of sulfate reduction was achieved due to the presence of non-target PHCs. They concluded that some forms of organic matter, specifically alkanes and alkylated aromatic hydrocarbons, were being degraded and the lack of benzene biodegradation likely resulted from metabolic interference from these organic compounds. Only four samples from the C depth interval had toluene concentrations (20 to 2,700 µg/L) sufficient to allow quantification of both carbon and hydrogen isotopes (**Figure 7b**). The remainder of the samples collected from the C depth interval (except MP4C on Day 309) showed carbon enrichment for toluene ranging from 0.7 ‰ to 11.6 ‰ (**Table SI-3**), suggesting

that toluene biodegradation was occurring. Toluene at MP3C on Day 0 showed enrichment in hydrogen isotope ($\Delta\delta^{13}C$ = 0.3‰, $\Delta\delta^{2}H$ = 28.6 ‰) while MP4C was depleted in hydrogen isotope ($\Delta\delta^{13}C$ = -0.3 ‰, $\Delta\delta^{2}H$ = -30.2‰) as carbon isotopic values were similar. On the other hand, an extremely high carbon and hydrogen isotopic enrichment was observed on Day 700 in samples collected from MP2C ($\Delta\delta^{13}C$ = +2.0 ‰, $\Delta\delta^{2}H$ = +74.7 ‰) and MP3C ($\Delta\delta^{13}C$ = +10.5 ‰, $\Delta\delta^{2}H$ = +442.3 ‰). These samples were collected during Irrigation Event-2 and these isotopic enrichments in toluene suggest that the mobilization of retained sulfate played a role in stimulating toluene biodegradation at C depth interval and/or toluene degraded during ongoing biodegradation at shallower depth was advanced downward with infiltrating water. Carbon and hydrogen isotope data for benzene in samples collected from MW9 (250 to 1,000 µg/L) were very similar to the estimated source signature, except for Day 309 sample which was isotopically depleted in both ^{13}C and ^{2}H as compared to the estimated source signature **(Figure 7c)**. Conversely, significant carbon and hydrogen isotopic enrichments were observed for toluene in all samples collected from MW9 (22 to 56 µg/L, see **Figure 7d**) except for carbon on Day 1058. These isotopic enrichment values ranged from $\Delta\delta^{13}C$ = +4.5 ‰, $\Delta\delta^{2}H$ = +157.6 ‰ (for Day 0) sample to $\Delta\delta^{13}C$ = +8.9 ‰, $\Delta\delta^{2}H$ = +352.7 ‰ (for Day 470). The maximum isotopic values for carbon and hydrogen in toluene at MW9 are higher than those for B depth interval but less than those for C depth interval due to blending of groundwater.

Biomarkers

Genes: *abcA* transcripts, which are associated with anaerobic biodegradation of benzene (Abu Laban et al., 2010; Bouchard et al., 2018a), were detected between 2.7×10^{3} and 9.4×10^{4} copies/L at the C depth interval on Day 1058, indicating active anaerobic benzene

biodegradation. $bssA_{srb}$ transcripts, which are associated with biodegradation of one or more TEX constituents under sulfate-reducing conditions (Elshahed et al., 2001; Bouchard et al., 2018a; Shayan et al., 2018), were detected during each sampling event at MW9, indicating anaerobic catabolism of one or more of these compounds (**Figure SI-6**). Biodegradation under sulfate reducing conditions is further demonstrated by the detection of *dsrB* at MW9 between 5×10^6 and 2×10^7 copies mRNA/L (**Figure SI-6**). The gene *dsrB* is known to encode for dissimilatory sulfate reductase (Bouchard et al., 2018a).

Metabolites: Benzylsuccinate concentrations (a metabolite of toluene during biodegradation under anaerobic conditions) in samples collected from MW9 were below quantification limit on Day 0 and Day 1058 but ranged between 9 and 17 µg/L on Day 470, Day 644 and Day 756 (**Figure SI-6**). These biomarker data provide additional support to conclude that anaerobic biodegradation of toluene was occurring when sulfate was present at MW9. 2-methylbenzylsuccinate, which is a metabolite of anaerobic biodegradation of xylene, was also detected at Day 644 and Day 756 (40 and 72 µg/L, respectively) further indicating that xylenes were undergoing anaerobic biodegradation (Bouchard et al., 2018a).

Impact of Sulfate Application on Methanogenesis

During the 8 years before this sulfate land application study was initiated, the average background dissolved methane concentration (data from conventional monitoring wells) ranged from 3.6 mg/L (Day 0) to below detection (<0.002 mg/L) (**Figure 8**). Along with detections of dissolved methane, enriched ^{13}C-DIC at Day 0 (0.3‰, 3.5‰ and 4.5‰ at the B depth interval, the C depth interval and MW9) indicates methanogenesis was occurring prior to sulfate application (Landmeyer et al. 1996; Teramoto et al. 2020). Following sulfate

application, methane concentrations were higher within the study area than in the conventional monitoring wells sampled outside of the study area that were not part of this study but routinely monitored for site management. Following the addition of sulfate, the average methane concentrations at the B and C depth intervals within the study area increased from 3.3 mg/L on Day 0 to ~5.3 mg/L by Day 756. In contrast, a slight decrease in methane concentration at MW9 (from 6.2 mg/L on Day 0 to 4.4 mg/L on Day 756) was observed. MW9 straddles the B, C and D depth intervals and consistently high sulfate concentrations (160 to 270 mg/L from Day 0 to Day 756) were detected in MW9. The slight decrease in methane concentrations at MW9 could possibly be due to the dominance of sulfate reduction over methanogenesis, as corroborated by the relatively depleted ^{13}C-DIC (from 4.5‰ on Day 0 to -16.3‰ on Day 756). However, depletion in sulfate concentrations by Day 1058 clearly corresponds with an increase in methane concentration to 11 mg/L at the B and C depth intervals and to 8.7 mg/L at MW9. On average, (between the B and C depth intervals and MW9) methane concentrations on Day 1058 were ∼3 times higher than the background methane concentrations at Day 0. Between Day 756 and Day 1058, ^{13}C-DIC was enriched by 2.4 to 4.8‰ suggesting that methanogenesis was re-established and influenced mineralization of PHCs upon sulfate depletion. These observations are consistent with other studies where methanogenesis became the dominant biodegradation process once sulfate was depleted (Landmeyer et al., 1996; Shayan et al., 2018). The sustained increase in methane concentrations once sulfate was depleted indicates that methanogenesis was potentially more effective by Day 1058 in comparison with the background methanogenic conditions prior to or without sulfate application. These results support the hypothesis that sulfate reducers can potentially enrich the syntrophic microbial ecosystem that is responsible for the breakdown of complex PHCs and intermediates (Vogt et al., 2011; Siegert et al., 2011; Gieg et

al., 2014). Increase in methane concentrations and a positive shift of δ^{13}C-DIC values as sulfate was expended after Day 756 provide evidence that sulfate-induced syntrophic contribution to the microbial ecosystem may have enhanced the rate of methanogenesis and, therefore, of bulk PHC depletion. To the authors' knowledge, this is the first field study, which indicates the syntrophic benefit of enhancing methanogenesis following sulfate application.

Summary and Implications

Following surface application of gypsum, breakthrough of sulfate was confirmed in the vadose and saturated zones, but sulfate transport was impacted (delay with respect to bromide due to sulfate reduction) and sulfate (and bromide) retained in the vadose zone. Soil cores collected after 780 days indicated that ~45% of the applied sulfate was retained in the vadose zone which was remobilized by eight weeks of irrigation. The retention of sulfate (and bromide) enabled greater interaction with PHCs predominantly occurring in the shallower finer-grained vadose zone soil. Stable isotope analyses of ^{34}S-SO_4^{2-} provided clear evidence that sulfate reduction occurred both in the vadose zone and in the groundwater particularly at shallow depths where significant concentrations of PHCs were present. Presence of elevated sulfide and high Fe^{2+} to Fe^{3+} ratio in the vadose zone indicated that sulfate reduction to sulfide and consequent precipitation of sulfide minerals occurred. Corresponding depletion of ^{13}C-DIC confirmed that as sulfate was reduced, PHCs underwent complete mineralization. CSIA and biomarker data confirmed enhanced biodegradation of both benzene and toluene, and that toluene biodegradation occurred under sulfate-reducing conditions. Enhanced biodegradation of benzene was either insignificant in the presence of other PHCs (e.g., TEX) at the B depth interval or was occurring but was muted due to masking by fresh benzene dissolution. Benzene at the C depth interval showed significant isotopic enrichment of carbon

and hydrogen strongly indicating anaerobic biodegradation of benzene where TEX concentrations were low or negligible. The isotopic enrichment for hydrogen in benzene in multiple groundwater samples was generally greater than the upper bound of the expected isotopic enrichment for anaerobic biodegradation of benzene reported in the literature. The data for benzene isotope fractionation under well-defined redox conditions (e.g., those typically implemented at the lab-scale) is limited compared to toluene and, therefore, less confidence can be assigned to this expected isotopic zone for benzene degrading under sulfate-reducing conditions or under methanogenic conditions. It is noted that the isotope enrichment values in the literature are based on lab studies which may not be fully representative of syntrophic interactions that may be possible under actual field conditions.

As sulfate was depleted, DIC became strongly enriched in ^{13}C suggesting a return to methanogenic conditions. Methane concentrations within the study area increased by ∼3 times as compared to the pre-sulfate application conditions suggesting that syntrophic benefits from the application of sulfate may continue through enhancement of the rate of methanogenesis even after sulfate is expended. The multiple lines of evidence approach including diagnostic tools were used in this study to complement standard groundwater analyses and arrive at meaningful conclusions which would not have been possible with BTEX concentration trends alone. Short-screened multilevel monitoring locations at different depth intervals were shown to enhance the value of diagnostic tools and generated a better understanding of vertical heterogeneities in PHC and sulfate distribution than that provided by the long-screened conventional monitoring well.

Overall, the multiple lines of evidence demonstrate that surface application of gypsum followed by precipitation and / or irrigation-induced infiltration is a viable method to enhance biodegradation of a PHC-impacted smear zone. This method was especially effective in

delivering sulfate to the fine-grained zone below the water table (the B depth interval), which may be difficult using solution-based injection methods, recirculation or reliance on advection. A lower-permeability zone often contains a higher mass of PHC and tends to act as a long-term source as the natural depletion rates are slower due to a lack of electron acceptors. Sulfate application in this manner was not only shown to be impacting PHC biodegradation in the saturated zone, but active sulfate reduction was concomitant with PHC presence in the vadose zone as well. This implies that sulfate land application can potentially be used to enhance NSZD. The results of this study also suggest that in the presence of a persistent residual LNAPL, multiple applications of sulfate would be required to degrade overall PHC mass and reduce concentrations of other hydrocarbons (e.g., TEX), and reach remedial objectives for specific compounds of interest such as benzene. At other sites with relatively weathered PHC source (i.e., depleted in other competing PHCs) or a small PHC source, BTEX degradation following sulfate application is expected to occur faster. Depending upon site conditions, active irrigation of the treatment area should be considered to augment natural precipitation and to enhance the dissolution and infiltration of applied salts. Since PHCs in the vadose zone also consume sulfate, breakthrough of sulfate in groundwater should not be treated as the sole metric for assessing sulfate transport to groundwater. Use of a conservative tracer like bromide applied in conjunction with sulfate can assist in demonstrating infiltration of applied salts. Performance monitoring should be supported by multiple lines of evidence approach that can include CSIA of target compounds, and stable isotope analysis of sulfate and DIC.

Dedication

We dedicate this manuscript to Eugene (Gene) L. Madsen, Professor of Microbiology at Cornell University who passed away unexpectedly in 2017. Gene was part of our multidisciplinary research team comprised of collaborators from Switzerland, Canada and the United States. As the lone environmental microbiologist among numerous hydrogeologists, geochemists and engineers, Gene had an unenviable task of ensuring that we all appreciated the complex microbe world. He was collaborative, kind, generous, humorous, and a true scholar. Gene had meticulous attention to detail and outstanding writing skills. We hope Gene would not be disappointed with our microbiology discussion in this manuscript since, unfortunately, it did not benefit from Gene's careful touches.

Acknowledgements

The authors thank Gene Choquette and Henry Stremlau (Chevron Environmental Management and Real Estate Company), and Dianne Burnia, Michael Winkler and Joe Shoulders (Stantec) for their support and collaboration throughout the planning and implementation of the study. We are very grateful to Jim Barker (Professor Emeritus, University of Waterloo), Eric Daniels and Daniel Segal (Chevron Technical Center), Felipe Solano (University of Waterloo) and Daniel Bouchard (University of Neuchatel) for their assistance with initial design of this study. We also thank Chris De Rito (Cornell University) for his assistance with the biomarker analyses. Financial support for this investigation was provided by Chevron.

Supporting Information

Additional Supporting Information may be found in the online version of this article. Supporting Information is generally not peer reviewed.

Sections

Figures

Tables

References

Aelion, C.E., P.E. Höhener, D.E. Hunkeler, and R.E. Aravena. 2009. *Environmental Isotopes in Biodegradation and Bioremediation*. Boca Raton: CRC Press.

Aggarwal, P.K., M.E. Fuller, M.M. Gurgas, J.F. Manning, and M.A. Dillon. 1997. Use of Stable Oxygen and Carbon Isotope Analyses for Monitoring the Pathways and Rates of Intrinsic and Enhanced in Situ Biodegradation. *Environmental Science & Technology* 31 no. 2: 590-596.

Anderson, R., and D. Lovley. 2000. Anaerobic bioremediation of benzene under sulfate-reducing conditions in a petroleum contaminated aquifer. *Environmental Science & Technology*, no. 34: 2261– 2266.

Batlle-Aguilar, J., S. Brouyère, A. Dassargues, B. Morasch, D. Hunkeler, P. Höhener, L. Diels, K. Vanbroekhoven, P. Seuntjens, and H. Halen. 2009. Benzene dispersion and natural attenuation in an alluvial aquifer with strong interactions with surface water. *Journal of Hydrology* 369 no. 3: 305-317.

Batlle-Aguilar, J., B. Morasch, D. Hunkeler, and S. Brouyère. 2014. Benzene Dynamics and Biodegradation in Alluvial Aquifers Affected by River Fluctuations. *Groundwater* 52 no. 3: 388-398.

Bekins, B.A., F.D. Hostettler, W.N. Herkelrath, G.N. Delin, E. Warren, and H.I. Essaid. 2005. Progression of methanogenic degradation of crude oil in the subsurface. *Environmental Geosciences Journal* 12 no. 2: 139-152.

Bolliger, C., P. Höhener, D. Hunkeler, K. Häberli, and J. Zeyer. 1999. Intrinsic bioremediation of a petroleum hydrocarbon-contaminated aquifer and assessment of mineralization based on stable carbon isotopes. *Biodegradation* 10 no. 3: 201-217.

Bombach, P., H.H. Richnow, M. Kästner, and A. Fischer. 2010. Current approaches for the assessment of in situ biodegradation. *Applied Microbiology and Biotechnology* 86 no. 3: 839-852.

Bouchard, D., D. Hunkeler, E.L. Madsen, T. Buscheck, E. Daniels, R. Kolhatkar, C.M. DeRito, R. Aravena, and N. Thomson. 2018a. Application of Diagnostic Tools to Evaluate Remediation Performance at Petroleum Hydrocarbon-Impacted Sites. *Groundwater Monitoring & Remediation* 38 no. 4: 88-98.

Bouchard, D., M. Marchesi, E.L. Madsen, C.M. DeRito, N.R. Thomson, R. Aravena, J.F. Barker, T. Buscheck, R. Kolhatkar, E.J. Daniels, and D. Hunkeler. 2018b. Diagnostic Tools to Assess Mass Removal Processes During Pulsed Air Sparging of a Petroleum Hydrocarbon Source Zone. *Groundwater Monitoring & Remediation* 38 no. 4: 29-44.

Braeckevelt, M., A. Fischer, and M. Kästner. 2012. Field applicability of Compound-Specific Isotope Analysis (CSIA) for characterization and quantification of in situ contaminant degradation in aquifers. *Applied Microbiology and Biotechnology* 94 no. 6: 1401-1421.

Buscheck, T., Mackay, D., Paradis, C., Schmidt, R., de Sieyes, N., 2019. Enhancing microbial sulfate reduction of hydrocarbons in groundwater using permeable filled borings, *Groundwater Monitoring & Remediation* 39 no. 3: 48-60.

Chakraborty, R., and J.D. Coates. 2004. Anaerobic degradation of monoaromatic hydrocarbons. *Applied Microbiology and Biotechnology* 64 no. 4: 437-446.

Charng, M.K., Voice, T.C. and Criddle, C.S. 1993. Kinetics of competitive inhibition and cometabolism in the biodegradation of benzene, toluene, and p-xylene by two Pseudomonas isolates. Biotechnol. Bioeng. 41(11), 1057-1065.

Conrad, M.E., P.F. Daley, M.L. Fischer, B.B. Buchanan, T. Leighton, and M. Kashgarian. 1997. Combined 14C and δ13C Monitoring of in Situ Biodegradation of Petroleum Hydrocarbons. *Environ SciTechnol* 31 no. 5: 1463-1469.

Cunningham, J.A., H. Rahme, G.D. Hopkins, C. Lebron, and M. Reinhard. 2001. Enhanced In Situ Bioremediation of BTEX-Contaminated Groundwater by Combined Injection of Nitrate and Sulfate. *Environ Sci Technol* 35 no. 8: 1663-1670.

El-Naas, M.H., J.A. Acio, and A.E. El Telib. 2014. Aerobic biodegradation of BTEX: Progresses and Prospects. *JEnviron Chem Eng* 2 no. 2: 1104-1122.

Elshahed, M.S., Gieg, L.M., McInerney, M.J., and Suflita, J.M. 2001. Signature Metabolites Attesting to the In Situ Attenuation of Alkylbenzenes in Anaerobic Environments. *Environ Sci Technol* 35 no. 4, 682–689.

Fayemiwo, O., M. Daramola, and K. Moothi. 2017. BTEX compounds in water - future trends and directions for water treatment. *Water SA* 43: 602-613.

Feisthauer, S., Seidel, M., Bombach, P., Traube, S., Knöller, K., Wange, M., Fachmann, S., and Richnow, H. H., 2012. Characterization of the relationship between microbial degradation processes at a hydrocarbon contaminated site using isotopic methods, *Journal of Contaminant Hydrology*, 133, 17–29.

Fischer, A., I. Herklotz, S. Herrmann, M. Thullner, S.A.B. Weelink, A.J.M., Stams, M. Schlomann, H.-H. Richnow, and C. Vogt, 2008. Combined carbon and hydrogen isotope fractionation analysis for elucidating benzene biodegradation pathways. *Environmental Science & Technology*, 42 (12), 4356 – 4363

Fischer, A., M. Gehre, J. Breitfeld, H.-H. Richnow, and C. Vogt. 2009. Carbon and hydrogen isotope fractionation of benzene during biodegradation under sulfate-reducing

conditions: a laboratory to field site approach. *Rapid Communications in Mass Spectrometry* 23 no. 16: 2439-2447.

Foght, J. 2008. Anaerobic biodegradation of aromatic hydrocarbons: pathways and prospects. *J Mol Microbiol Biotechnol* 15 no. 2-3: 93-120.

Garg, S., Newell, C.J., Kulkarni, P.R., King, D.C., Adamson, D.T., Irianni-Renno, M., and Sale, T., 2017. Overview of Natural Source Zone Depletion: Processes, Controlling Factors, and Composition Change. *Groundwater Monitoring & Remediation* 37 no. 3: 62-81.

Gibson, D.T., and R.E. Parales. 2000. Aromatic hydrocarbon dioxygenases in environmental biotechnology. *Current Opinion in Biotechnology* 11 no. 3: 236-243.

Gieg, L.M., S.J. Fowler, and C. Berdugo-Clavijo. 2014. Syntrophic biodegradation of hydrocarbon contaminants. *Current Opinion in Biotechnology* 27: 21-29.

Griebler, C., M. Safinowski, A. Vieth, H.H. Richnow, and R.U. Meckenstock. 2004. Combined Application of Stable Carbon Isotope Analysis and Specific Metabolites Determination for Assessing In Situ Degradation of Aromatic Hydrocarbons in a Tar Oil-Contaminated Aquifer. *Environmental Science & Technology* 38 no. 2: 617-631.

Hunkeler, D., P. Höhener, S. Bernasconi, and J. Zeyer. 1999. Engineered in situ bioremediation of a petroleum hydrocarbon-contaminated aquifer: assessment of mineralization based on alkalinity, inorganic carbon and stable carbon isotope balances. *Journal of Contaminant Hydrology* 37 no. 3: 201-223.

Hutchins, S.R., D.E. Miller, and A. Thomas. 1998. Combined Laboratory/Field Study on the Use of Nitrate for in Situ Bioremediation of a Fuel-Contaminated Aquifer. *Environmental Science & Technology* 32 no. 12: 1832-1840.

Irianni-Renno, M., Akhbari, D., Olson, M.R., Byrne, A.P., Lefevre, E., Zimbron, J., Lyverse, M., Sale, T.S., De Long, S.K, 2016. Comparison of bacterial and archaeal communities in depth-resolved zones in an LNAPL body, *App Microbiol Biotechnol*, 100 (7), 3347-60.

Jeannottat, S., and D. Hunkeler. 2012. Chlorine and Carbon Isotopes Fractionation during Volatilization and Diffusive Transport of Trichloroethene in the Unsaturated Zone. *Environmental Science & Technology* 46 no. 6: 3169-3176.

Kennedy, L.G., J.W. Everett, K.J. Ware, R. Parsons, and V. Green. 1998. Iron and sulfur mineral analysis methods for natural attenuation assessments. *Bioremediation Journal* 2 no. 3-4: 259-276.

Knöller, K., C. Vogt, H.-H. Richnow, and S.M. Weise. 2006. Sulfur and Oxygen Isotope Fractionation during Benzene, Toluene, Ethyl Benzene, and Xylene Degradation by Sulfate-Reducing Bacteria. *Environmental Science & Technology* 40 no. 12: 3879-3885.

Knöller, K., C. Vogt, , Feisthauer, S., S.M. Weise, H. Weiss, H.-H., Richnow. 2008. Sulfur cycling and biodegradation in contaminated aquifers: insights from stable isotope investigations, *Environmental Science & Technology*, 42 (21), 7807–7812.

Kolhatkar, R., and M. Schnobrich. 2017. Land Application of Sulfate Salts for Enhanced Natural Attenuation of Benzene in Groundwater: A Case Study. *Groundwater Monitoring & Remediation* 37 no. 2: 43-57.

Laban, A. N., D. Selesi, T. Rattei, P. Tischler, and R.U. Meckenstock. 2010. Identification of enzymes involved in anaerobic benzene degradation by a strictly anaerobic iron-reducing enrichment culture. *Environmental Microbiology* 12 no. 10: 2783-2796.

Landers, D.H., M.B. David, and M.J. Mitchell. 1983. Analysis of Organic and Inorganic Sulfur Constituents in Sediments, Soils and Water. *International Journal of Environmental Analytical Chemistry* 14 no. 4: 245-256.

Landmeyer, J.E., D.A. Vroblesky, and F.H. Chapelle. 1996. Stable Carbon Isotope Evidence of Biodegradation Zonation in a Shallow Jet-Fuel Contaminated Aquifer. *Environ Sci Technol* 30 no. 4: 1120-1128.

Liu, J.B., T. Amemiya, Q. Chang, X. Xu, and K. Itoh. 2011. Real-time reverse transcription PCR analysis of trichloroethylene-regulated toluene dioxygenase expression in Pseudomonas putida F1. *Journal of Environmental Science and Health, Part B* 46 no. 4: 294-300.

Mancini, S.A., Devine, C.E., Elsner, M., Nandi, M.E., Ulrich, A.C., Edwards, E.A., and Sherwood Lollar, B. 2008. Isotopic evidence suggests different initial reaction mechanisms for anaerobic benzene biodegradation. *Environ Sci Technol* 42: 8290–8296.

McGuire, J.T., D.T. Long, and D.W. Hyndman. 2005. Analysis of recharge-induced geochemical change in a contaminated aquifer. *Ground Water* 43 no. 4: 518-530.

Meckenstock, R.U., M. Boll, H. Mouttaki, J.S. Koelschbach, P. Cunha Tarouco, P. Weyrauch, X. Dong, and A.M. Himmelberg. 2016. Anaerobic Degradation of Benzene and Polycyclic Aromatic Hydrocarbons. *Journal of Molecular Microbiology and Biotechnology* 26 no. 1-3: 92-118.

Meckenstock, R.U., M. Elsner, C. Griebler, T. Lueders, C. Stumpp, J. Aamand, S.N. Agathos, H.-J. Albrechtsen, L. Bastiaens, P.L. Bjerg, N. Boon, W. Dejonghe, W.E. Huang, S.I. Schmidt, E. Smolders, S.R. Sørensen, D. Springael, and B.M. van Breukelen. 2015. Biodegradation: Updating the Concepts of Control for Microbial Cleanup in Contaminated Aquifers. *Environmental Science & Technology* 49 no. 12: 7073-7081.

Meckenstock, R.U., and H. Mouttaki. 2011. Anaerobic degradation of non-substituted aromatic hydrocarbons. *Current Opinion in Biotechnology* 22 no. 3: 406-414.

Morasch, B., D. Hunkeler, J. Zopfi, B. Temime, and P. Höhener. 2011. Intrinsic biodegradation potential of aromatic hydrocarbons in an alluvial aquifer – Potentials and limits of signature metabolite analysis and two stable isotope-based techniques. *Water Research* 45 no. 15: 4459-4469.

OSU, 2011. Gypsum as an Agricultural Amendment – General Use Guidelines, Ohio State University, 2011

Otton, J.K., and R.A. Zielinski. 2000. Simple techniques for assessing impacts of oil and gas operations on Federal Lands - A field evaluation at Big South Fork National River and Recreation Area, Scott County, Tennessee (online edition). US Geological Survey.

Palau, J., M. Marchesi, J.C.C. Chambon, R. Aravena, À. Canals, P.J. Binning, P.L. Bjerg, N. Otero, and A. Soler. 2014a. Multi-isotope (carbon and chlorine) analysis for fingerprinting and site characterization at a fractured bedrock aquifer contaminated by chlorinated ethenes. *Science of The Total Environment* 475: 61-70.

Palau, J., O. Shouakar-Stash, and D. Hunkeler. 2014b. Carbon and Chlorine Isotope Analysis to Identify Abiotic Degradation Pathways of 1,1,1-Trichloroethane. *Environmental Science & Technology* 48 no. 24: 14400-14408.

Parisi, V.A., Brubaker, G.R., Zenker, M.J., Prince, R.C., Gieg, L.N., da Silva, M.L.B., Alvarez, P.J.J., Suflita, J.M., 2009. Field metabolomics and laboratory assessments of anaerobic intrinsic bioremediation of hydrocarbons at a petroleum-contaminated site, *Microbial Biotechnology*, 2(2), 202-212.

Ponsin, V., T.E. Buscheck, and D. Hunkeler. 2017. Heart-cutting two-dimensional gas chromatography–isotope ratio mass spectrometry analysis of monoaromatic hydrocarbons in complex groundwater and gas-phase samples. *Journal of Chromatography A* 1492: 117-128.

Ponsin, V., J. Maier, Y. Guelorget, D. Hunkeler, D. Bouchard, H. Villavicencio, and P. Höhener. 2015. Documentation of time-scales for onset of natural attenuation in an aquifer treated by a crude-oil recovery system. *Science of The Total Environment* 512-513: 62-73.

Prommer, H., B. Anneser, M. Rolle, F. Einsiedl, and C. Griebler. 2009. Biogeochemical and Isotopic Gradients in a BTEX/PAH Contaminant Plume: Model-Based Interpretation of a High-Resolution Field Data Set. *Environmental Science & Technology* 43 no. 21: 8206-8212.

Prosser, C.M., A.D. Redman, R.C. Prince, M.L. Paumen, D.J. Letinski, and J.D. Butler. 2016. Evaluating persistence of petroleum hydrocarbons in aerobic aqueous media. *Chemosphere* 155: 542-549.

Rodríguez-Fernández, D., C. Torrentó, J. Palau, M. Marchesi, A. Soler, D. Hunkeler, C. Domènech, and M. Rosell. 2018. Unravelling long-term source removal effects and chlorinated methanes natural attenuation processes by C and Cl stable isotopic patterns at a complex field site. *Science of The Total Environment* 645: 286-296.

Scanlon, B.R., R.C. Reedy, R.L. Baumhardt, and G. Strassberg. 2008. Impact of deep plowing on groundwater recharge in a semiarid region: Case study, High Plains, Texas. *Water Resources Research* 44 no. 7.

Scholl, M.A., I.M. Cozzarelli, and S.C. Christenson. 2006. Recharge processes drive sulfate reduction in an alluvial aquifer contaminated with landfill leachate. *Journal of Contaminant Hydrology* 86 no. 3: 239-261.

Schroth, M.H., J. Kleikemper, C. Bolliger, S.M. Bernasconi, and J. Zeyer. 2001. In situ assessment of microbial sulfate reduction in a petroleum-contaminated aquifer using

push–pull tests and stable sulfur isotope analyses. *Journal of Contaminant Hydrology* 51 no. 3: 179-195.

Schürmann, A., M.H. Schroth, M. Saurer, S.M. Bernasconi, and J. Zeyer. 2003. Nitrate-consuming processes in a petroleum-contaminated aquifer quantified using push–pull tests combined with 15N isotope and acetylene-inhibition methods. *Journal of Contaminant Hydrology* 66 no. 1: 59-77.

Siegert, M., Cichocka, D., Herrmann, S., Grundger, F., Feisthauer, S., Richnow, H.-H., Springael, D., and Kruger, M., 2011. Accelerated methanogenesis from aliphatic and aromatic hydrocarbons under iron- and sulfate-reducing conditions", *Microbiol Lett*, 315 (2011) 6-16.

Shayan, M., N.R. Thomson, R. Aravena, J.F. Barker, E.L. Madsen, M. Marchesi, C.M. DeRito, D. Bouchard, T. Buscheck, R. Kolhatkar, and E.J. Daniels. 2018. Integrated Plume Treatment Using Persulfate Coupled with Microbial Sulfate Reduction. *Groundwater Monitoring & Remediation* 38 no. 4: 45-61.

Solano, F.M., M. Marchesi, N.R. Thomson, D. Bouchard, and R. Aravena. 2018. Carbon and Hydrogen Isotope Fractionation of Benzene, Toluene, and o-Xylene during Chemical Oxidation by Persulfate. *Groundwater Monitoring & Remediation* 38 no. 4: 62-72.

Spence, M.J., S.H. Bottrell, S.F. Thornton, H.H. Richnow, and K.H. Spence. 2005. Hydrochemical and isotopic effects associated with petroleum fuel biodegradation pathways in a chalk aquifer. *Journal of Contaminant Hydrology* 79 no. 1: 67-88.

Sra, K.S., N.R. Thomson, and J.F. Barker. 2013. Persulfate Treatment of Dissolved Gasoline Compounds. *Journal of Hazardous, Toxic, and Radioactive Waste* 17 no. 1: 9-15.

Teramoto, E.H., C. Vogt, Mp. P. M. Baessa, L. Polese, A. U. Soriano, H. K. Chiang, and H. H. Richnow, 2020. Dynamics of hydrocarbon mineralization characterized by isotopic

analysis at a jet-fuel-contaminated site in subtropical climate. *Journal of Contaminant Hydrology*, 234, 103684.

Thullner, M., Centler, F., Richnow, H.-H., and Fischer, A., 2012. Quantification of organic pollutant degradation in contaminated aquifers using compound specific stable isotope analysis – Review of recent developments. *Organic Geochemistry*, 42, 1440-1460.

Toth, C. R. A., Luo, F., Bawa, N., Webb, J., Guo, S., Dworatzek, S., and Edwards, E.A., 2021. Anaerobic Benzene Biodegradation Linked to the Growth of Highly Specific Bacterial Clades, *Environmental Science & Technology* 55, 7970-7980.

Torrentó, C., J. Palau, D. Rodríguez-Fernández, B. Heckel, A. Meyer, C. Domènech, M. Rosell, A. Soler, M. Elsner, and D. Hunkeler. 2017. Carbon and Chlorine Isotope Fractionation Patterns Associated with Different Engineered Chloroform Transformation Reactions. *Environmental Science & Technology* 51 no. 11: 6174-6184.

USEPA, 1995. Light nonaqueous phase liquids, United States Environmental Protection Agency, Ground Water Issue, EPA/540/S-95/500.

USEPA. 2008. A Guide for Assessing Biodegradation and Source Identification of Organic Ground Water Contaminants using Compound Specific Isotope Analysis (CSIA). United States Environmental Protection Agency.

Van Stempvoort, D.R., J. Armstrong, and B. Mayer. 2007. Microbial reduction of sulfate injected to gas condensate plumes in cold groundwater. *Journal of Contaminant Hydrology* 92 no. 3: 184-207.

Varjani, S.J. 2017. Microbial degradation of petroleum hydrocarbons. *Bioresource Technology* 223: 277-286.

Viollier, E., P.W. Inglett, K. Hunter, A.N. Roychoudhury, and P. Van Cappellen. 2000. The ferrozine method revisited: Fe(II)/Fe(III) determination in natural waters. *Applied Geochemistry* 15 no. 6: 785-790.

Wanner, P., R. Aravena, J. Fernandes, M. BenIsrael, E.A. Haack, D.T. Tsao, K.E. Dunfield, and B.L. Parker. 2019. Assessing toluene biodegradation under temporally varying redox conditions in a fractured bedrock aquifer using stable isotope methods. *Water Research* 165: 114986.

Weelink, S.A.B., M.H.A. van Eekert, and A.J.M. Stams. 2010. Degradation of BTEX by anaerobic bacteria: physiology and application. *Reviews in Environmental Science and Bio/Technology* 9 no. 4: 359-385.

Wei, Y., N.R. Thomson, R. Aravena, M. Marchesi, J.F. Barker, E.L. Madsen, R. Kolhatkar, T. Buscheck, D. Hunkeler, and C.M. DeRito. 2018. Infiltration of Sulfate to Enhance Sulfate-Reducing Biodegradation of Petroleum Hydrocarbons. *Groundwater Monitoring & Remediation* 38 no. 4: 73-87.

Wiedemeier, T.H., H.S. Rifai, C.J. Newell, and J.T. Wilson. 1999. *Natural Attenuation of Fuels and Chlorinated Solvents in the Subsurface*. New-York: John Wiley & Son.

Wilson, J.T., C. Adair, H. White, and R.L. Howard. 2016. Effect of Biofuels on Biodegradation of Benzene and Toluene at Gasoline Spill Sites. *Groundwater Monitoring & Remediation* 36 no. 4: 50-61.

Biographical Sketches

Kanwartej S. (Kammy) Sra, Ph.D., P.Eng. (PEO), corresponding author, is Lead Environmental Engineer (Remediation Specialist) at Chevron Technical Center, 1400 Smith St., Houston, TX 77002; (713) 372-2165, Kammy.Sra@chevron.com

Violaine Ponsin, Ph.D., is Assistant Professor at Department of Earth and Atmospheric Sciences, Université du Québec à Montréal, 405 Rue Sainte-Catherine Est, Montréal, QC, Canada H2L 2C4; (514) 987-3000 ext 3375, ponsin.violaine@uqam.ca

Ravi Kolhatkar, Ph.D., MBA, is Senior Remediation Specialist at Chevron Energy Technology Company, 1400 Smith St, Houston, Texas 77002; (713) 372-2126; kolhatrv@chevron.com

Daniel Hunkeler, Ph.D., is Professor and Director of the Centre for Hydrogeology and Geothermics (CHYN), University of Neuchâtel, Emile-Argand 11 CH-2000 Neuchâtel, Switzerland; +41(0) 32 718 25 60; daniel.hunkeler@unine.ch

Neil R. Thomson, Ph.D., P.Eng. (PEO), Professor at the Department of Civil and Environmental Engineering, University of Waterloo, 200 University Avenue West, Waterloo, ON, Canada N2L 3G1; (519) 888 4567 ext 32111, neil.thomson@uwaterloo.ca

Eugene L. Madsen, Ph.D., Deceased, was Professor in the Department of Microbiology, Cornell University, 123 Wing Drive, Ithaca, NY 14853.

Timothy Buscheck, M.S., P.E., is Emeritus Chevron Fellow at Chevron Technical Center, 6001 Bollinger Canyon Road, San Ramon, CA 94583; timbuscheck@gmail.com

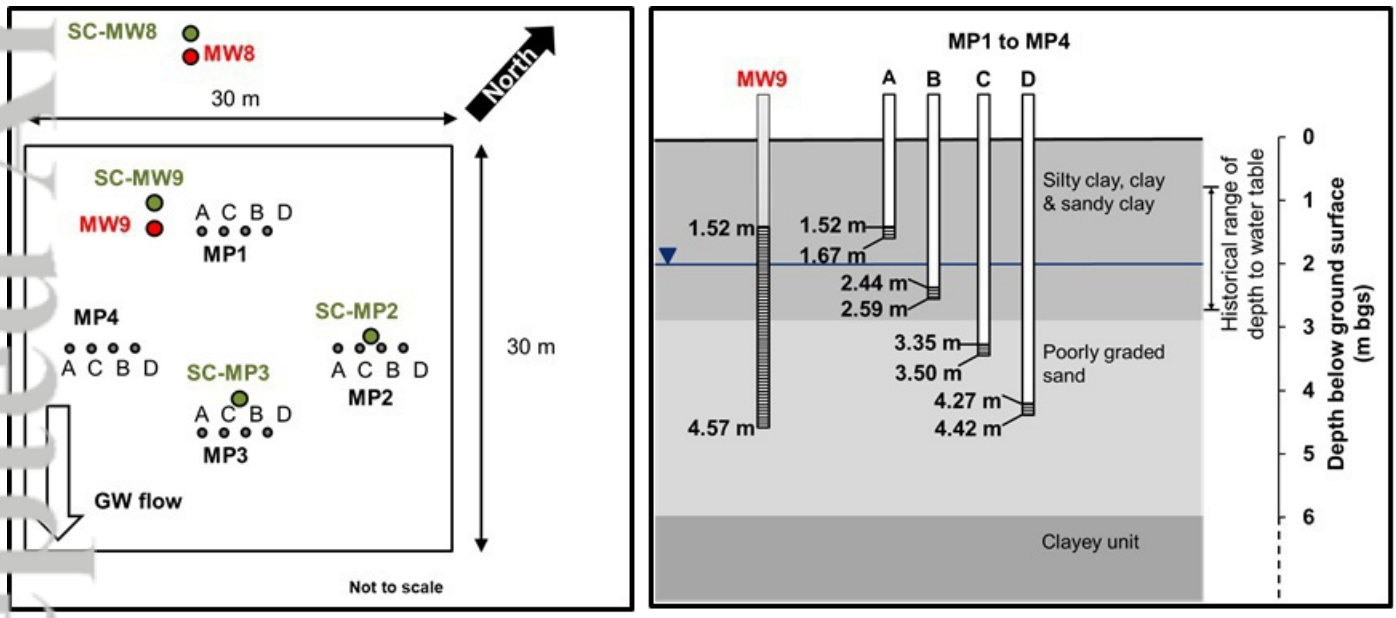

GWMR_12547_Figure1.jpg

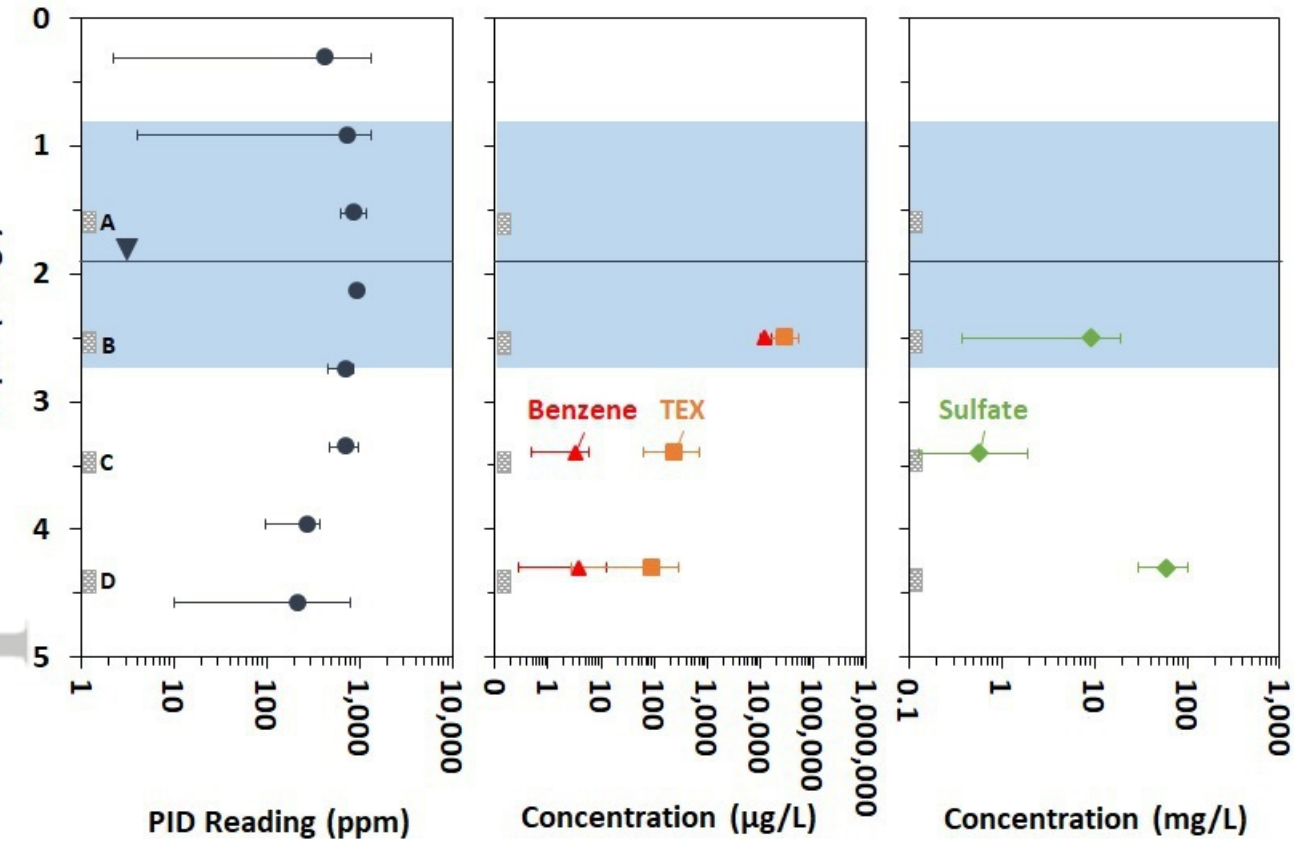

GWMR_12547_Figure2.jpg

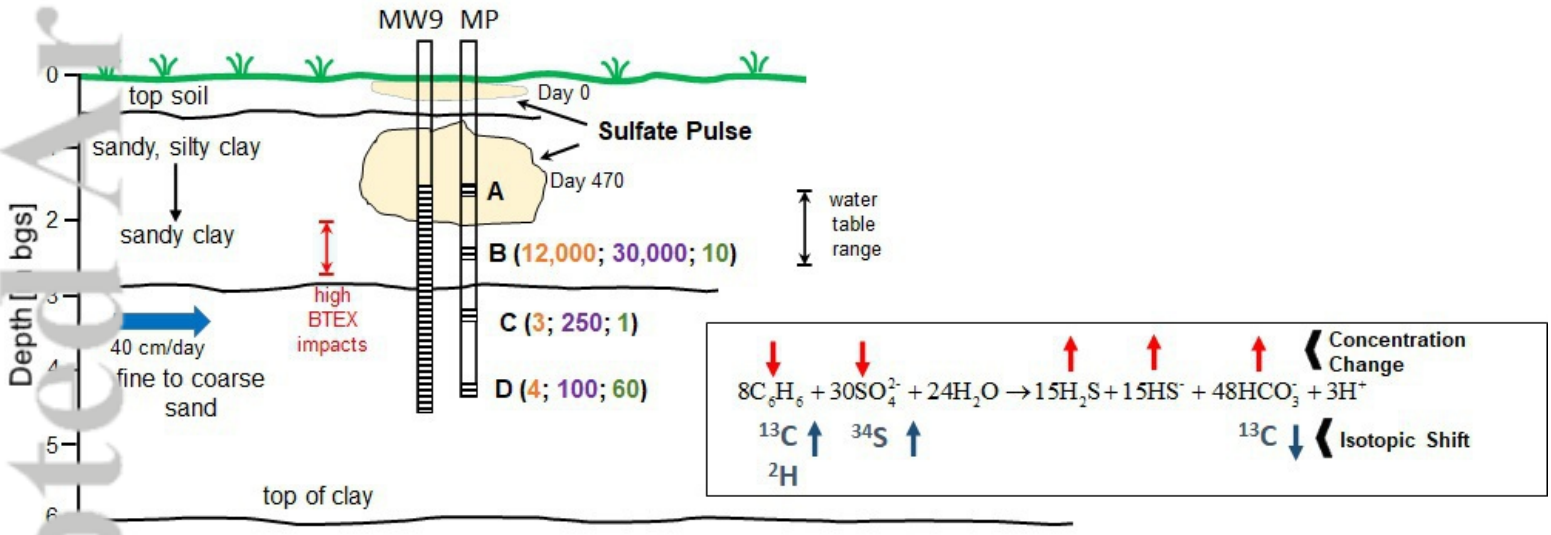

Concentration at baseline at depth intervals B, C and D
(e.g., Benzene – 12,000 µg/L; TEX - 30,000 µg/L; $SO4^{2-}$ - 10 mg/L)

GWMR_12547_Figure3.jpg

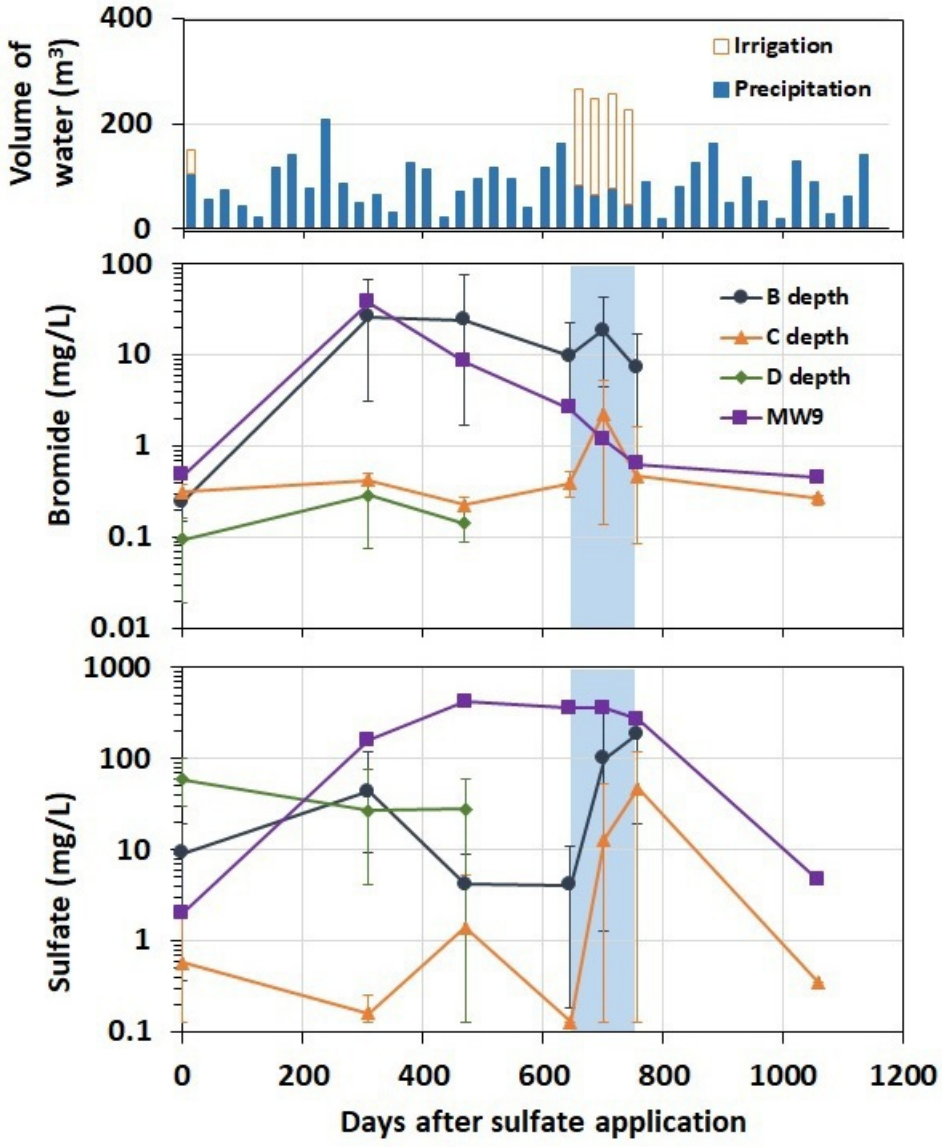

GWMR_12547_Figure4.jpg

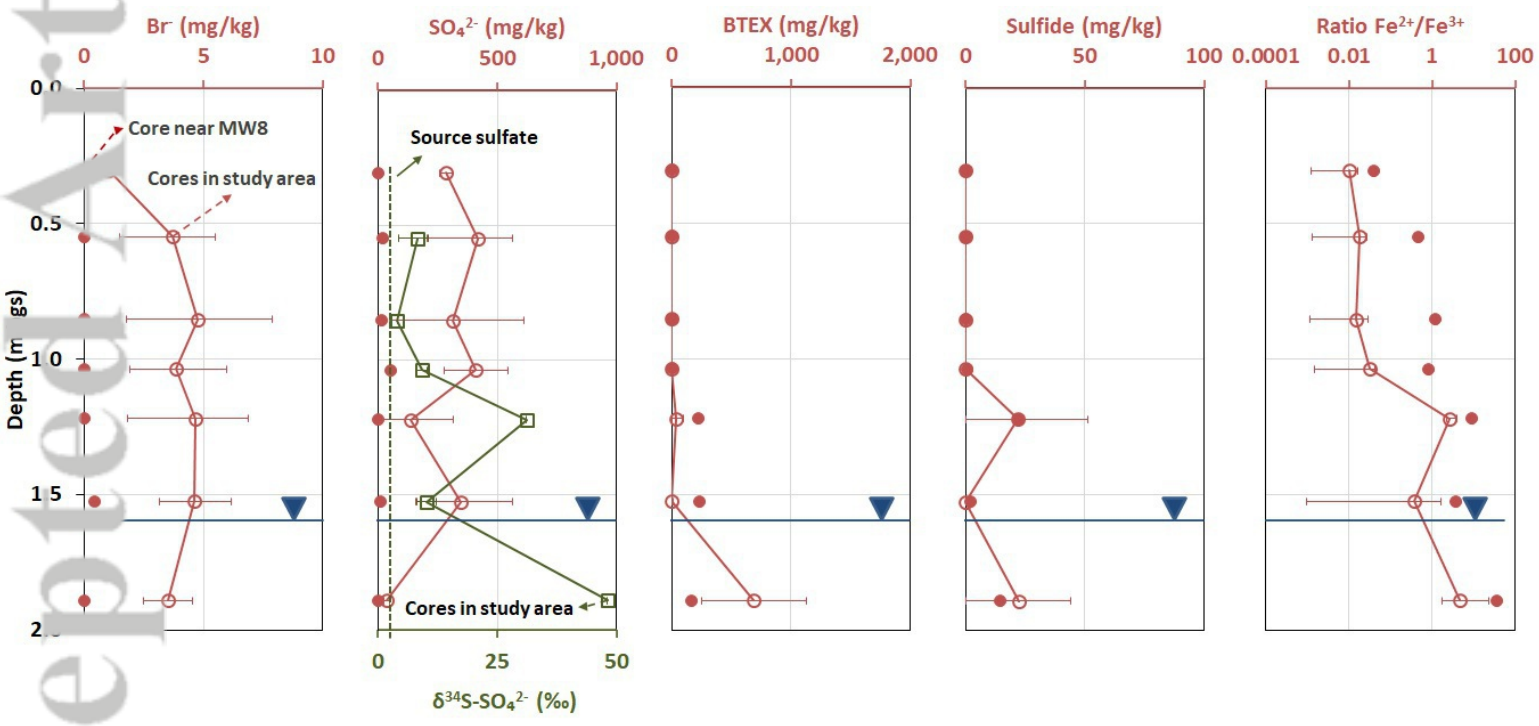

GWMR_12547_Figure5.jpg

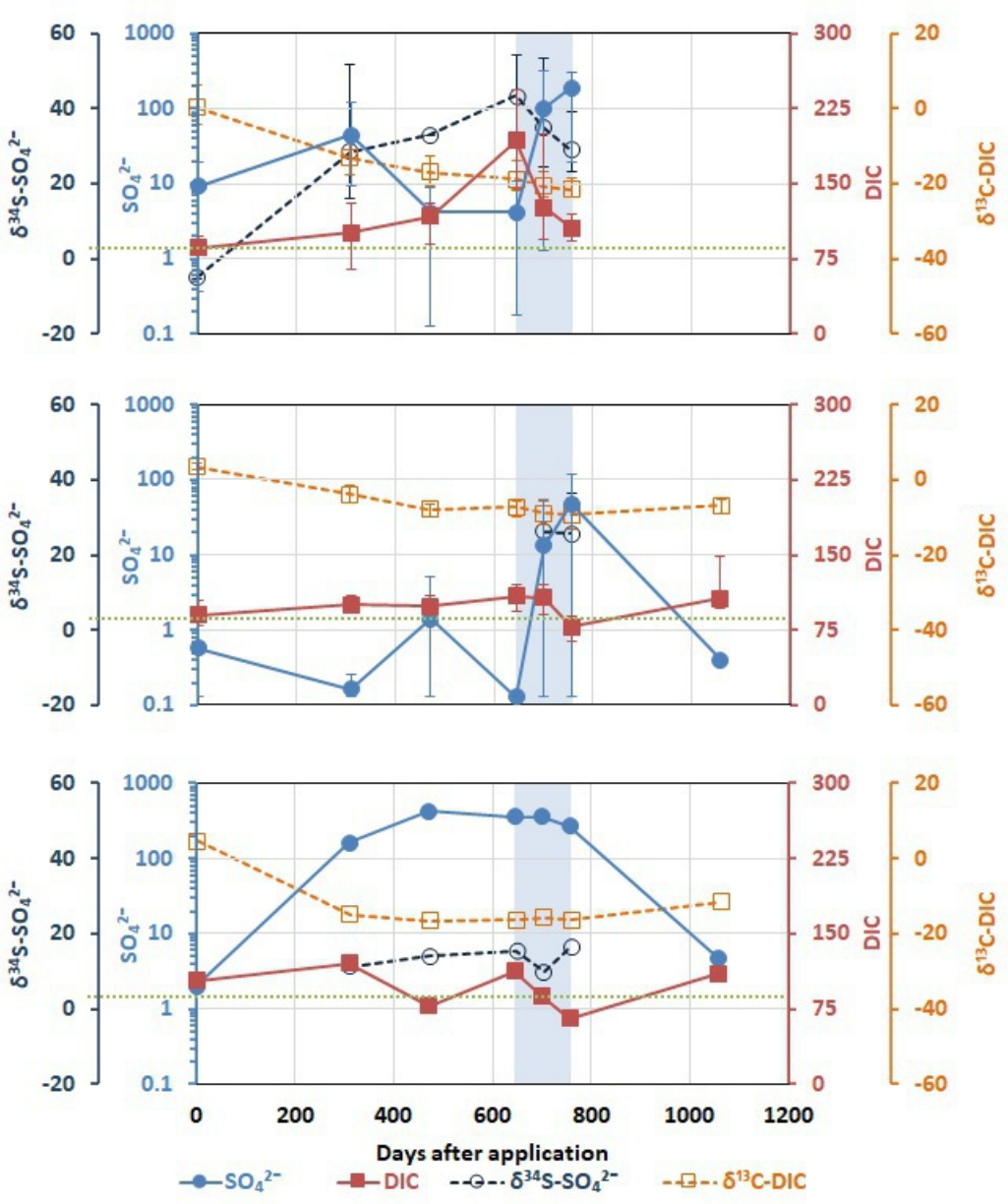

GWMR_12547_Figure6.jpg

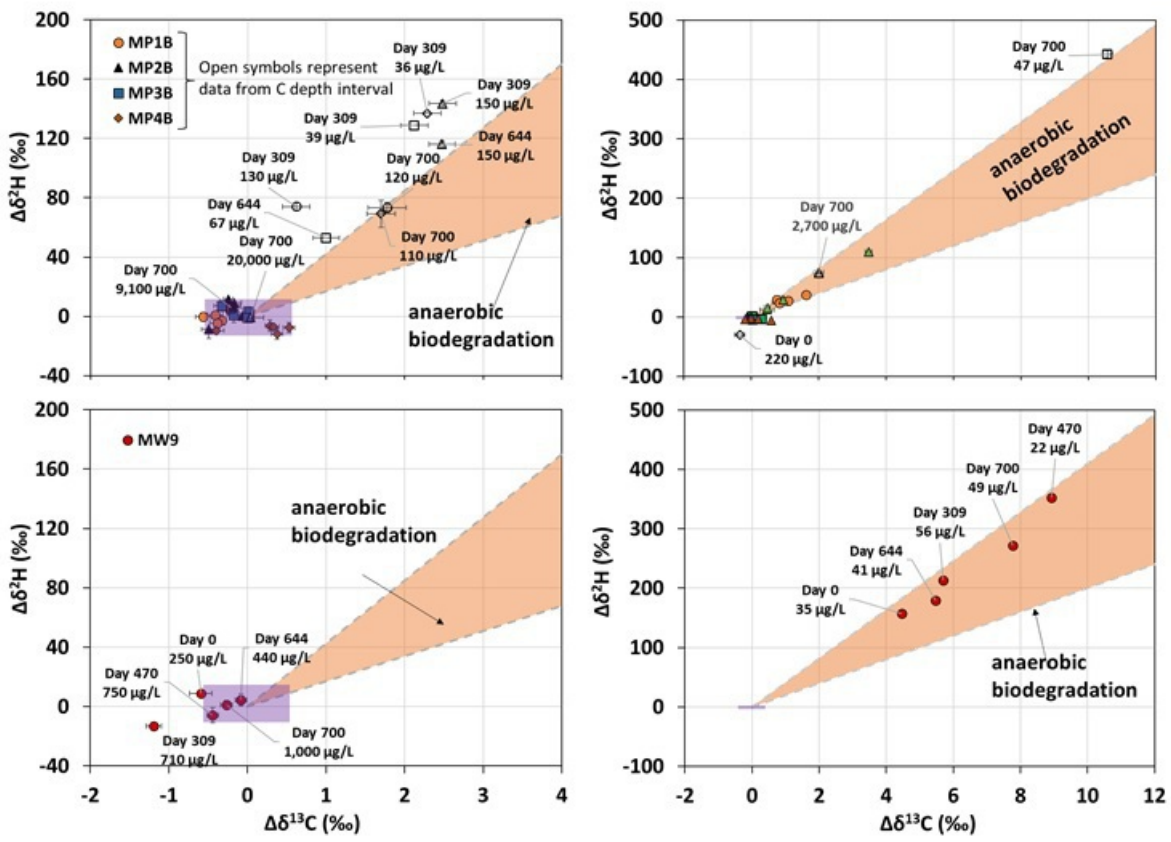

GWMR_12547_Figure7.jpg

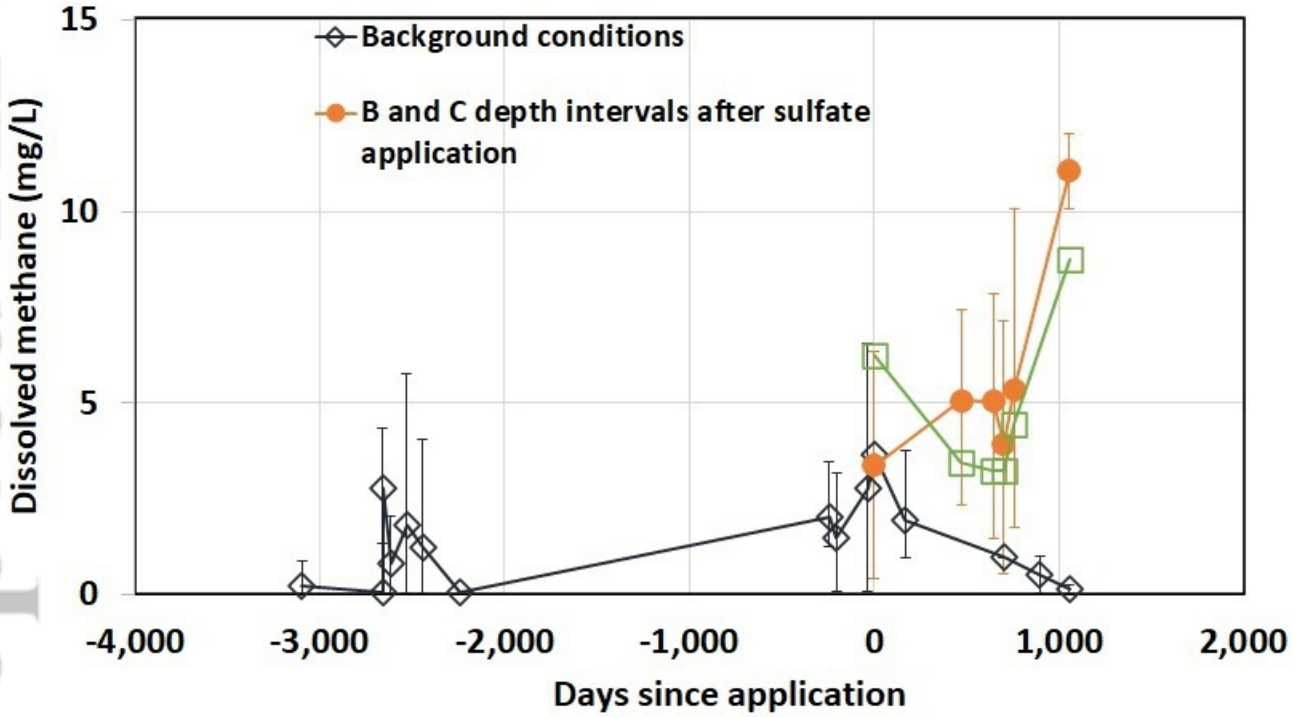

GWMR_12547_Figure8.jpg